Perpetua

THE UAH JOURNAL OF UNDERGRADUATE RESEARCH

VOLUME 4 | ISSUE 2 | SPRING 2020

THE UNIVERSITY OF ALABAMA IN HUNTSVILLE

PERPETUA

Perpetua

UAH Journal of Undergraduate Research

Volume 4, Issue 2

THE UNIVERSITY OF
ALABAMA IN HUNTSVILLE

Perpetua Staff

Editor in Chief: Benjamin Tran

Assistant Editor in Chief: Maxwell Fox

Communications Director: Ashleigh Oliver

Managing Editors:

Anna Hargrove

Dr. Christy Jeffcoat

Editorial Staff:

Kerri Balance

Jaiden Gann

Brianna Gamez

Christa Howell

Michael Joseph

Maris Onushi

Minh Tran

Katie Weaver

Eli Williams

Faculty Advisors:

Mr. David Cook (Undergraduate Research & Honors College)

Dr. Yu Lei (College of Engineering - Department of Chemical Engineering)

Dr. Hamsa Mahafza (College of Education - Department of Curriculum and Instruction)

Letter from the Editor

It is with great pleasure that I present the latest issue of *Perpetua* to you, the students, faculty, researchers, and associates of the University of Alabama in Huntsville as well as the curious minds outside the UAH system. On behalf of *Perpetua*, I would like to extend a sincere expression of gratitude for the generous contribution of all the graduate students, faculty, administrators, and alumni who given their time towards the growth and realization of this publication.

Perpetua has now, for three years, been driven with a mission to represent the excellency of the undergraduate research community. A great but worthy responsibility. We are once again indebted to the researchers who have entrusted their work to us and extended their confidence to represent their research in the best possible manner.

Since the Fall of 2016, *Perpetua* has provided a platform for researchers to release their work to the public. But these have indeed been unusual times. Particularly this semester as of late has tried the patience of our authors, reviewers, editorial staff, and faculty. However, as we close this semester, we are reminded that we not only carry a heavy responsibility to our authors but also to our up-and-coming students. Such is evidenced by the students and faculty on the staff who understand that *Perpetua* serves a greater purpose than broadcasting the accomplishments of an undergraduate community. And as I look back on the past year and the year before that and even then, the year preceding, I feel a bittersweet smile forming on my face. Because as this year's chapter sets, another, one more glorious than the last, awaits.

It is with great pleasure that I present to you, the readers, the latest issue from *Perpetua*. pages, we hope that you yourselves are inspired to pursue your own research and join this talented community of undergraduates at UAH.

It has been an absolute pleasure,

Benjamin Tran
Editor in Chief
Perpetua

Special Thanks

Perpetua is a collaborative effort and publication would be impossible without the support of numerous individuals and organizations across UAH and throughout the greater Huntsville research and outreach community. We offer special thanks to all who have contributed their time, expertise, financial support, and hard work to *Perpetua.* A few of our biggest contributors are recognized below.

First and foremost, we would like to thank the undergraduate student researchers for entrusting us with the privilege and the responsibility of promoting their work. We thank the various faculty and staff who serve as sponsors to undergraduate research and to the Research and Creative Experience for Undergraduates for providing resources and opportunities and who likewise support and promote undergraduate research.

We thank the Office of Student Life for providing ample opportunities to promote Perpetua and its purpose. We thank the Office of Academic Affairs for enabling us to reach as many members of the UAH community as possible. We would also like to thank Dr. William Wilkerson and the UAH Honors College for their commitment to providing additional financial support to *Perpetua*. Next, we would like to extend our thanks to our faculty advisors: Mr. David Cook, Dr. Yu Lei, and Dr. Hamsa Mahafza, who have consistently provided exceptional insight and guidance to our editorial staff since our inception.

Finally, we thank every UAH graduate student and faculty member who served as a reviewer for one of the manuscripts featured in this issue. Without such individuals volunteering their time and expertise, *Perpetua* would not be able to provide our services to the UAH community.

Table of Contents

The Usefulness of Achilles Tendon Length in Predicting Jump Potential in Male Collegiate Basketball and Track & Field Athletes

Mohammad Alrefai, Richard Claytor & Brianna New
Department of Kinesiology

Abstract **–** Tendon mechanical properties and composition allow them to play a role in force production. One such tendon, the Achilles tendon, is the thickest and strongest tendon in the body and has been studied sparsely in regard to resting length and vertical jump performance. **PURPOSE**: To determine the correlation between Achilles tendon length (ATL) and vertical jump output. **METHODS**: Twenty-one males (19.33±1.39 years, 78.48±10.31 kg, 183.43±7.33 cm) were recruited from UAH men's track & field and basketball teams. Participants were scheduled a one-time session consisting of anthropometrics, ATL measurement, and vertical jump assessment. The ATL measurement was performed bilaterally by having the participant lay in the prone position on a table with their shoes off and leg flexed. The researcher added resistance to the plantar flexed foot for observation of the tendon. ATL was measured from the calcaneal tuberosity to the insertion on the gastrocnemius. ATL was reported as the mean of the bilateral measurements. Vertical jump height was assessed for standing jump and running countermovement jump using a vertical jump testing device. Participants completed two trials for both jumps, and a third trial was taken if necessary. Pearson's r was used to calculate correlation and significance was set at $p \leq 0.05$. **RESULTS**: A significant moderate-to-large positive correlation was found between ATL and standing vertical jump ($r=0.433$, $p=0.0497$). A non-significant, low correlation was observed for ATL and running vertical jump ($r=.284$, $p=.2126$). **CONCLUSION**: The positive relationship between ATL and vertical jump performance shows a potential tool in predicting jump potential.

Keywords: Achilles, Jump, Vertec, Correlation, Relationship Between Achilles Tendon Length and Jump Performance in Male Collegiate Basketball and Track & Field Athletes

I. Introduction

Tendons are the attachment between muscle and bone (Lichtwark & Wilson, 2005). They help transmit force produced by the muscle to the bone (Kirkendall & Garrett, 1997). Optimal mechanical properties for force transmission are the high tensile strength, resiliency, stiffness, and number of type II glycolytic fibers and type I collagen (Doral, Alam, Bozkurt, Turhan, Atay, Dönmez, and Maffuli., 2010; Wong and Kiel., 2019). The rigid properties allow for more efficient transfer of force between the muscle and bone (Doral et al., 2010). For example, the low elasticity and high collagen composition allows for rapid force production (Wong & Kiel., 2019).

One such tendon, Achilles tendon (AT), is the most powerful tendon in the body (Doral et al., 2010). According to Edama et al. (2016), the AT attaches near the calcaneal tuberosity on the calcaneus, giving cause to its anatomical name, the calcaneal tendon. The aponeurosis of the gastrocnemius and soleus conjoin at the low end of the calf constituting the superior end of the AT (Doral et al., 2010; Dixon, 2009). When jumping, the lower calf muscles and the AT go through a stretch shortening cycle to provide lower body force. According to (Larsen, 2018), the AT provides a medium for the force created by the body to be translated to the ground.

During loading, the gastrocnemius and soleus contract as force is applied to the minimally stretched AT. When the muscles are unable to contract any more, the AT recoils and pulls on the calcaneus to produce downward force. According to Bayliss et al. (2016), the lead jumping leg in athletes had a superior AT Young's modulus (ability to resist changes in length) compared to their lead leg. This means jump training may lead to physiological adaptations allowing for jump-trained athletes to be a more uniform and appropriate group to test than their more variable non-athlete counterparts. A problem that is posed is that it is unknown whether the Achilles tendon length plays a role in vertical jump Young and Michael (2002) state that Achilles tendon length (ATL) is determined by genetics. If a correlation between ATL and vertical jumping ability is observed, it would both show that Achilles Tendon length plays a role in jump output and highlight another way in which genetics can affect jump performance.

The purpose of this study was to determine if a relationship between ATL and vertical jumping ability exists. We hypothesized that athletes with longer ATL would have a higher vertical jump than those who have a shorter ATL.

II. Methods

Participants

Twenty-one healthy males aged 18-24 who are current athletes from The University of Alabama in Huntsville basketball and track & field teams were recruited for the study. Athletes with debilitating injuries were excluded from the study for safety. Athletes with debilitating injuries were excluded from the sample because of its negative effect on jump performance. All participants were instructed to abstain from exercise for 24 hours prior to testing.

Table 1. *Subject Demographics*

Variable	M ± SD
Age (yrs)	19.33 ± 1.39
Height (cm)	183.43 ± 7.33
Weight (kg)	78.48 ± 10.31

Note. Yrs = Years

Instrumentation

The Vertec, by Sports Imports, was used to analyze vertical jump height in Spragins Hall. The Vertec is a measuring tool for jump height that is used as a tool of reference for taking the difference between the maximum standing reach and maximum jumping reach. According to Leard et al. (2007), the Vertec is highly correlated (r = 0.906) with the analysis of jump height using a 3-camera motion analysis system, which is considered the gold standard.

Achilles Tendon Length Measurement

In adequate lighting, the designated researcher palpated the superior aspect of the calcaneus/heel until the insertion of the Achilles tendon was identified (Del Buono, Chan, & Maffulli, 2013). The identified location was marked at the most superior point on the calcaneus with a 0.8mm marker. While researchers pushed against the subject's plantar flexed foot, the highest visible point of the muscle-tendon insertion near the gastrocnemius was also marked (Del Buono et al., 2013). The researcher measured the distance between the two locations in mm. The ATL was measured bilaterally to ensure a consistent and accurate measurement.

Maximal Standing Vertical Jump Height

The measurements for vertical jump height took place on the basketball court or in the racquetball courts in Spragins Hall. To measure vertical jump height with the Vertec, standing reach was first measured in comfortable athletic footwear. Subjects stood with both feet flat on the ground with both legs and torso straight. They reached up with a straight arm, wrist, and hand, and their standing reach was determined by the highest vane touched without jumping. Vanes on the Vertec were then raised to measure jump height. Subjects used the same arm for standing reach as they did with their jumps.

The subject jumped off two feet straight up as high as possible, with a straight arm, and tapped the Vertec device. No shuffle steps, side steps, drop steps, or gather steps were allowed. Participants made two jumps, and a third was given if a higher jump was achieved during the second jump. The standing vertical jump is the difference, in inches, between the

standing reach and the jump reach. Only the maximal vertical jump height was recorded.

Maximal Running Vertical Jump Height

Maximum approach distance was measured from 15 feet from the Vertec. Starting within the 15-foot range, they took as many steps toward the Vertec as necessary to acquire a maximum vertical jump. Everyone was required to start within the 15-foot arc, and each athlete was instructed to perform the jump with a two-foot takeoff. The subject completed two vertical jumps. If on the second attempt, a greater jump height was reached, a third attempt was awarded. The running vertical jump height was measured in the same manner as the standing jump height.

Design and Analysis

This study was a cross-sectional study in which data collection for every participant involved a single 10-15-minute session. After recording the data, a Pearson's correlation was performed to determine whether a significant relationship existed between ATL and vertical jumping ability. ATL was divided by the subject's height to normalize the data; then a Pearson's correlation was performed between the normalized ATL and vertical jump height. Significance was set at $p \leq 0.05$.

III. Results

A significant moderate-to-large Pearson's correlation coefficient was found between ATL and standing jump ($r = 0.433$, $p = 0.0497$). The correlation between ATL and running jump was found to be insignificant at ($r = 0.284$, $p = 0.2126$). We also normalized measures by dividing height to see if relative ATL had a significant relationship with jump height. A nonsignificant relationship was found between both normalized ATL and standing jump ($r = 0.408$, $p = 0.0663$) and normalized ATL and running jump ($r = 0.283$, $p = 0.2145$) (Hopkins, 2007).

Table 2. *Mean and Standard Deviation for ATL and Jump Height*

Variable	(M ± SD)
Avg ATL (mm)	219.87 ± 29.31
Standing Jump (in)	25.05 ± 3.70
Running Jump (in)	29.64 ± 3.84
Normalized ATL	8.48 ± 1.16

Note. ATL = Achilles tendon length
Avg = Average

Table 3. *Correlations between ATL, Jump Height, and ATL/Height*

Variable	1	2	3	4
1. Average ATL	—	—	—	—
2. Standing Jump	0.433*	—	—	—
3. Running Jump	0.283	—	—	—
4. Average ATL/height	—	0.408	0.283	—

Note. ATL = Achilles tendon length $*p \leq 0.05$

Figure 1. *ATL vs. Jump Height - Note*: ATL = Achilles tendon length

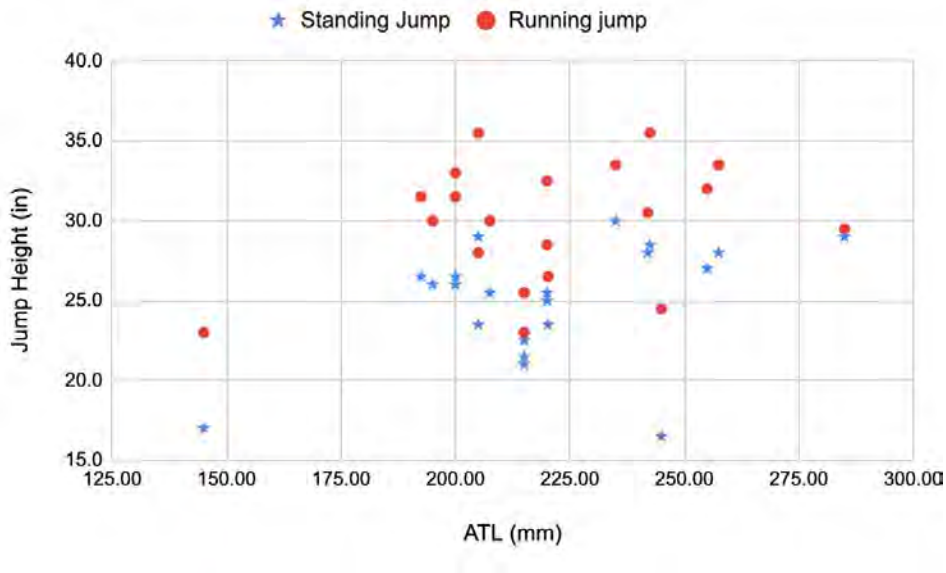

IV. Discussion

The purpose of this study was to determine whether a relationship between ATL and vertical jump height exists. The hypothesis of this research was that a positive correlation existed between ATL and vertical jump height. This hypothesis was partially supported. While the relationship between standing vertical jump height and ATL had a significant relationship with a moderate-to-large positive correlation, no significant correlation was observed with ATL and running jump.

No studies to date have measured resting ATL and its relationship to vertical jump height. However, studies have examined tendon elasticity and stiffness and their relationship to jump height. Muraoka, Muramatsu, Fukunaga, and Kanehisa (2005) showed that in individuals with greater muscular strength, the AT elongated less after equal loading than individuals with less muscular strength. At maximum voluntary isometric contraction, there were no significant differences between training status and elongation. However, Muraoka et al. (2005) used isometric force production, rather than dynamic activities such as jumping, therefore AT elongation across training status may vary during isotonic conditions. According to Bayliss et al. (2016), jumpers exhibited significantly greater Young's Modulus and AT stiffness in their jumping leg than their lead leg. The increase in stiffness and ability to resist changes in length after repetitive loads show a morphological training aspect in relation to jump height. Since all jumps were executed with a two-foot take off, inter-leg differences with the ATL and jump performance could not be assessed. In the current study, ATL was positively correlated to vertical jump height, but information about how resting ATL relates to stiffness, elongation, and force production and how this ultimately affects jump height is largely un-researched. Combining Bayliss' results with the present study, it can be concluded that both training and genetic factors affect jump height. Since ATL is largely based on genetics and Young's modulus, which can be improved through training, both have been shown to be positively correlated with vertical jump height, supporting the conclusion of the present study.

According to Tai, Wang, and Peng (2018), single-leg jumps resulted in greater stiffness and impulse than two-legged jumps. However, two-legged jumps still produced a greater force production and resulted in higher vertical jumps. Kirby, McBride, Haines, and Dayne (2011), analyzed squat depth and its relation to vertical jump height. They found that net vertical impulse was positively correlated to jump height in all squat depths studied. Squat depth in the present study was unaccounted for and may have affected the results. According to

Domire and Challis (2007), computer models showed that lower squat depths resulted in greater vertical displacement due to the longer ground contact time. However, recreational jump-trained athletes demonstrated increased displacement at their preferred squat depth rather than the deeper squat depth. In athletic settings such as basketball, a lower ground contact time is optimal due to the nature of the game. Therefore, the results from Domire and Challis may be due to the lack of practice of deeper countermovement and standing jumps.

Limitations

In a perfect setting, ATL measurements would be taken with an MRI. As the gold standard, it is far more accurate than a manual palpation of muscle insertion point (Chang & Miller, 2009). Manual palpation has been recognized as a reliable measurement, but has not been validated (Hansen, Barfod, & Kristensen, 2017). Due to the expensive nature of the MRI, it was not feasible to run one subject through an MRI, let alone 21 participants.

Another limitation experienced was the overall n-size of subjects. According to G-Power 3.1, an n-size of 333 would give more power to our study with $\beta = 0.80$ reducing the effect of outlier points (Faul, Erdfelder, Lang, & Buchner, 2007). Despite this study only involving 21 participants, it was an initial pilot investigation worthy of being expanded into a larger N-size.

An additional limitation was requiring participants to jump off of two feet. The reason they were required to jump off two-feet was to standardize the methods. Since a two-foot takeoff was required, both ATL measurements were taken. However, some participants prefer to conduct their running vertical off of one leg since that is what they have done throughout their athletic career or they are able to achieve a higher vertical jump off of one leg.

Future Directions

Future research could focus on comparing the manual ATL measurement with the gold standard for tendon imaging: MRI. Comparing ATL taken with an MRI to manual methods will help determine whether the measurements taken by the researchers are valid, in addition to highly reliable measurements.

Future studies could compare AT biomechanical properties such as Young's modulus, tendon stiffness, and changes in tendon length with resting ATL. With this information, there will be a better understanding of how the resting ATL compares with changes in ATL during loading, force production, and vertical jump height.

Finally, future studies can compare ATL with 1-leg and 2-leg running jumps. This will allow for a more inclusive study which accounts for jump preference, training history, and varying biomechanical properties, such as young's modulus.

V. Conclusion

We found that resting ATL and vertical jump height share a significant relationship during maximal standing vertical jump. Although the measurements were taken with reliable methodology, it is unknown whether the manual measurement is valid. This research will potentially provide more insight into the abilities of the AT and its relation to vertical jump height. Furthermore, ATL measurements may be useful as an evaluation tool to estimate the jump potential of athletes.

References

Bayliss, A. J., Weatherholt, A. M., Crandall, T. T., Farmer, D. L., McConnell, J. C., Crossley, K. M., & Warden, S. J. (2016). Achilles tendon material properties are greater in the jump leg of jumping athletes. Journal of musculoskeletal & neuronal interactions, 16(2), 105.

Chang, A., & Miller, T. T. (2009). Imaging of tendons. Sports health, 1(4), 293-300.

Del Buono, A., Chan, O., & Maffulli, N. (2013). Achilles tendon: functional anatomy and novel emerging models of imaging classification. International Orthopaedics, 37(4), 715-721.

Dixon, J. B. (2009). Gastrocnemius vs. soleus strain: how to differentiate and deal with calf muscle injuries. Current reviews in musculoskeletal medicine, 2(2), 74-77.

Domire, Z. J., & Challis, J. H. (2007). The influence of squat depth on maximal vertical jump performance. Journal of sports sciences, 25(2), 193-200.

Doral, M. N., Alam, M., Bozkurt, M., Turhan, E., Atay, O. A., Dönmez, G., & Maffulli, N. (2010). Functional anatomy of the Achilles tendon. Knee Surgery, Sports Traumatology, Arthroscopy, 18(5), 638-643.

Edama, M., Kubo, M., Onishi, H., Takabayashi, T., Yokoyama, E., Inai, T., ... & Kageyama, I. (2016). Structure of the Achilles tendon at the insertion on the calcaneal tuberosity. Journal of anatomy, 229(5), 610-614.

Faul, F., Erdfelder, E., Lang, A.-G., & Buchner, A. (2007). G*Power 3: A flexible statistical power analysis program for the social, behavioral, and biomedical sciences. Behavior Research Methods, 39, 175–191.

Hansen, M. S., Barfod, K. W., & Kristensen, M. T. (2017). Development and reliability of the Achilles Tendon Length Measure and comparison with the Achilles Tendon Resting Angle on patients with an Achilles tendon rupture. Foot and Ankle Surgery, 23(4), 275-280.

Hopkins, W. G., (2007, August 16). A Scale of Magnitudes for Effect Statistics. Retrieved from https://www.sportsci.org/resource/stats/effectmag.html.

Kirby, T. J., McBride, J. M., Haines, T. L., & Dayne, A. M. (2011). Relative net vertical impulse determines jumping performance. Journal of Applied Biomechanics, 27(3), 207-214.

Kirkendall, D. T., & Garrett, W. E. (1997). Function and biomechanics of tendons. Scandinavian journal of medicine & science in sports, 7(2), 62-66.

Larsen, A. V. (2018). Effect of increased Achilles tendon stiffness on Gastrocnemius and Soleus fascicle behavior (Master's thesis).

Leard, J. S., Cirillo, M. A., Katsnelson, E., Kimiatek, D. A., Miller, T. W., Trebincevic, K., & Garbalosa, J. C. (2007). Validity of two alternative systems for measuring vertical jump height. The Journal of Strength & Conditioning Research, 21(4), 1296-1299.

Lichtwark, G. A., & Wilson, A. M. (2005). In vivo mechanical properties of the human Achilles tendon during one-legged hopping. Journal of Experimental Biology, 208(24), 4715-4725.

Muraoka, T., Muramatsu, T., Fukunaga, T., & Kanehisa, H. (2005). Elastic properties of human Achilles tendon are correlated to muscle strength. Journal of Applied Physiology, 99(2), 665-669.

Tai, W. H., Wang, L. I., & Peng, H. T. (2018). Biomechanical Comparisons of One-Legged and Two-Legged Running Vertical Jumps. Journal of human kinetics, 64(1), 71-76.

Wong M, Kiel J. (2019). Anatomy, Bony Pelvis and Lower Limb, Achilles Tendon. [Updated 2018 Dec 6]. Retrieved from https://www.ncbi.nlm.nih.gov/books/NBK459362/.

Young, M., & Michael, L. (2002). A review on postural realignment and its muscular and neural components. British Journal of Sports Medicine, 9(12).

Analysis of the Activation of Upper Extremity Muscles During Various Chest Press Modalities

Jamison Christian, Sydney Gothart, Harrison Graham & Katelyn Barganier
Department of Kinesiology

Abstract **–** The path to increasing muscular strength begins with resistance training. Multiple variations of the bench press exist for strengthening the chest and shoulder musculature. All modalities serve an important role in strength training. PURPOSE: Determine the level of muscle activation of the anterior deltoid (AD), medial deltoid (MD), and pectoralis major (PM) during different bench press scenarios. METHODS: Twenty subjects (10 males,10 females; age = 24±2.99 years) with at least one year of resistance training were recruited. Six electromyographical sensors were placed bilaterally on the targeted muscles. Subjects performed a one-repetition maximum (1-RM) of dumbbell (DB) and barbell (BB) press during two sessions followed by six repetitions at an incline, flat, and decline position using 70% of their 1-RM. Mean peak values for muscle activation were analyzed for each variation. A repeated measures one-way analysis of variance was used to compare muscle activation patterns across conditions; significance was set at $p \leq 0.05$. RESULTS: AD activation was significantly higher during incline BB compared to decline BB/decline DB ($p \leq .019$). MD activation was significantly lower across all modalities when compared to AD ($p \leq .040$). PM activation was significantly lower during incline BB compared to decline DB ($p = .011$). CONCLUSION: Differences among AD and PM may have been due to the stability stipulation variations between DB/BB and the large biacromial breadth requirement. Lack of differentiation of muscle fibers within the PM during sensor placement could have led to lesser muscle activation recordings at a decline.

Keywords: muscle activation, 1-RM, resistance training

I. Introduction

The path to muscular fitness begins with resistance training programs. These programs vary by frequency, intensity, time, and type. A common measurement for upper body muscular strength is the bench press. While the standard flat barbell (BB) bench press is the hallmark for strength measurements, it also has multiple variations including incline, decline, dumbbell (DB), Smith machine, and unstable bases of support. The primary muscles responsible for the bench press movement are the pectoralis major (PM), anterior deltoid (AD), triceps brachii, and the medial deltoid (MD), with the MD acting as a stabilizer muscle (Jagessar, Gray, 2010).

Glass and Armstrong (1997) looked at variations of the bench press and how the musculature reacts to these variations in both incline and decline positions, while others like Jagessar and Gray (2010) analyzed grip position concluding that the maximum activation of the prime movers was recorded while subjects had a grip of 190% of their biacromial width. These studies vary in several ways. Some look at simply incline, decline, or flat bench (Glass & Armstrong, 1997) while others incorporate a variation such as the use of DBs (Saeterbakken, Tillaar, Fimland, 2010), Smith machine (Schick et al. 2010), or performing the exercise on an unstable surface. The common thread among these studies is the use of healthy and active male subjects. In this research study we incorporated DB, BB, incline, flat, and decline press exercises, while also utilizing both male and female subjects.

Female subjects have not been included in studies similar to this one in the past, likely because females typically have a larger amount of subcutaneous fat than men do, particularly in the chest region. This is seen as an obstacle when

performing studies due to the accuracy of the electromyography (EMG) recordings through the larger layer of fat. In a study about the effect of interelectrode distance of EMG signals in women and men, Tomita, Ando, Saito, Watanabe, and Akima hypothesized that EMG indices of vastus intermedius (VI) and vastus lateralis (VL) would differ between inter-electrode distances of 10 mm and 20 mm due to the greater subcutaneous fat thickness in women (Tomita et. al. 2015). There is a lack of research on the effect of breast tissue on EMG recordings in females, but the results of Tomita et al. showed that as long as the subject did not classify as obese according to body mass index (BMI), the subcutaneous fat levels would not affect the EMG signals, regardless of sex.

During the same study, Tomita et al. (2015) also hypothesized that EMG indices of VI and VL would differ between men and women with respect to differences in force levels. These differences would be due to the difference in anatomical structure variations between women and men affecting the interelectrode distances chosen for each subject. The results revealed that the frequency and amplitude of EMG signals at different levels of force by women and men are not affected by interelectrode distances. Even though interelectrode distances did not affect the outcome of this study, Williamson, Epstein, and Lombardo (1980) concluded the placement of electrodes is crucial in determining the accuracy of EMG results.

The main purpose of this study was to determine the level of muscular activation of the anterior deltoid (AD), medial deltoid (MD), and pectoralis major (PM) during different bench press scenarios. Through the use of EMG technology, we monitored and observed the muscular activity of the AD, MD, and PM while conducting BB bench press and DB press on an incline bench (+30°), a flat bench (0°), and a decline bench (-30°). We hypothesized that the greatest activation would be observed in the PM during the decline bench press and DB press. Also, we further hypothesized that an inverse relationship would exist between AD activation and PM activation. While in an inclined position, the AD muscles were expected to show more activation, and consequently less activation of PM. Correspondingly, during a declined position we expected a greater amount of activation in the PM and less activation in the AD. A secondary aim of this study was also to compare muscle activation levels between genders. The hypothesis for the secondary aim is that males will have higher muscle activation in the PM than females, and values for the AD and MD will show no significant differences.

II. Methods

Participants

Twenty college aged individuals (10 male & 10 female) were recruited to the Human Performance Laboratory for two testing occasions. Recorded subject characteristics appear in **Table 1**.

All subjects had a minimum of one year of resistance training experience as an inclusion factor for the study. All subjects reported having completed the BB bench press and/or DB press on average of once per week during the past year of training. All subjects were provided an informed consent form approved by the university's Institutional Review Board, and subjects were provided an opportunity to ask the investigators any questions related to the study prior to enrolling in the study. Written informed consent was obtained from each subject prior to the first data collection session. Subjects were excluded from the study if they had musculoskeletal pain, an illness, or injury that might reduce maximal effort during testing (Saeterbakken, 2010). Exclusion criteria also included individuals who classified as obese according to their body fat percentage. The American College of Sports Medicine classifies 20-29 year-old females with a body fat percentage greater than 30.5% and 20-29 year-old males with a body fat percentage greater than 24.9% as being in the very poor fitness category (2018).

Variable	Mean ± SD
Age	24 ± 2.99 years
Height	172.23 ± 10.69 cm
Mass	73.31 ± 17.06 kg
Body fat	17.79 ± 6.14%
Resistance training experience	6.1 ± 2.92 years

Table 1. *Overall Participant Characteristics*

Equipment

Equipment consisted of the Perform Better (PB) (Warwick RI) extreme half rack, PB extreme rubber bumper plates, a Lamar adjustable bench, PB extreme BB, and pro series PowerBlock DBs. Data was collected utilizing EMG technology (DATALITE WS1800 wireless EMG system). The data was then analyzed with SPSS (Chicago, IL) for calculating differences in muscular activation from all the training sessions.

Testing Procedures

Subjects visited the laboratory for two sessions during the study. The first meeting consisted of the completion of a pre-participation health screening, Physical Activity Readiness Questionnaire (PAR-Q), signing of an informed consent form, and collection of resting measurements. Subjects were randomly assigned a testing sequence to determine if BB or DB was tested during the first session, with the remaining condition being tested during the second laboratory session. An equal distribution between the use of BB and DB for the first or second session was utilized to account for the potential for learning effect and fatigue. The order of these conditions (BB, DB) was counterbalanced and the order of bench angle (+30°, 0°, -30°) were randomized to control for bias or fatigue effect. One repetition maximum (1RM) testing was conducted in accordance with National Strength and Conditioning Association (NSCA) guidelines (**Table 2**). Subjects were randomly assigned to their test order group.

1RM Testing Protocol	
Step #	Procedures
1	Instruct the athlete to warm up with a light resistance that easily allows 5 to 10 repetitions
2	Provide a 1-minute rest period
3	Estimate a warm up load that will allow the athlete to complete three to five repetitions by adding 10 to 20 pounds
4	Provide a 2-minute rest period
5	Estimate a conservative, near maximal load that will allow the athlete to complete 2 to 3 repetitions by adding 10 to 20 pounds
6	Provide a 2 to 4-minute rest
7	Make load increase: 10 to 20 pounds
8	Instruct the athlete to attempt a 1RM
9a	If the athlete was successful, provide a 2 to 4-minute rest period and return to step 7
9b	If the athlete failed, provide a 2 to 4-minute rest period, then decrease the load by subtracting 5 to 10 pounds and return to step 8

Table 2. *NSCA 1RM*

Once the 1RM of the subjects was established, the subjects completed six repetitions of 70% of 1RM at an incline, flat, and decline position. These bench angles were measured using an international standard goniometer (Glass, 1997). A minimum of 48 hours later, the same protocol as the first visit was used for the mode that was not previously tested. The longest time between sessions was seven days.

To avoid muscular fatigue, our subjects were required to refrain from any upper extremity training for at least 48 hours prior to testing (Lauver, J. D., Cayot, T. E., & Scheuermann, B. W. 2015). Research has shown that it is best to not have the subjects on a set routine for workouts. To get the most valid muscle activation readings, we randomized bench conditions between subjects (Lauver, J. D., Cayot, T. E., & Scheuermann, B. W. 2015). The standard recovery time between sets is five minutes to avoid fatigue (Lauver, J. D., Cayot, T. E., & Scheuermann, B. W. 2015). It has been shown that to record the most accurate muscle activity, momentum cannot be used to complete the lift. Only slow controlled movements with no bounce off the chest coming to a full extension were recorded (Newton, R. U., Murphy, A. J., Humphries, B. J., Wilson, G. J., Kraemer, W. J., & HaKkinen, K. , 1997).

Exercise Form

Per Clemons, & Aaron (1997), the grip width for maximum engagement of the PM was shown to be 190% of the biacromial width of the subject. Biacromial width was determined by measuring the distance between the acromion processes utilizing an anthropometer, multiplying by 1.90, and dividing by 2. This quotient was then measured out from the center of the bar on each side which gave us a standardized grip position for all subjects.

Subjects were required to complete all repetitions in a fluid movement pattern with no pause at the bottom, and they were not able to bounce the bar off the chest. Also, the subjects were required to reach full elbow extension to record a successful lift (Newton, 1997). The DBs were not allowed to touch at the top for the DB bench (Welch 2005). We used two spotters during BB and DB lifts to ensure safety and to stabilize the BB and DB before and after each lift.

Electromyography

EMG sensors were placed on the AD, MD, and PM, and muscle activation was measured, charted, and recorded. In conducting the methods of this study there were several factors to consider to

correctly detect an EMG signal and measurements. In a related article on the use of surface EMG in biomechanics, Luca (1997) shared some important factors to consider which were incorporated into the methods of this study. When measuring for EMG signals, the signals were recorded with maximum fidelity. Initiation and cessation times and the parameters for measuring amplitude and frequency were carefully analyzed to maintain accuracy (Luca, 1997). Causative factors, both intrinsic and extrinsic, such as incorrect location or misconfiguration of the sensors, excess tissue in between the muscle and the electrode, excess motor units during the contraction, and also excess blood flow within the muscle are factors that could possibly affect the EMG signal. Muscular force should be indicated and dealt with prior to any procedure being performed. These situations can bring inaccuracy to the data by either making the signal reading higher or lower than it actually is. For example, excess motor units during the contraction can cause a higher signal reading. In order to ensure consistent sensor placement the same investigators placed the sensors on the participants during each of the trials.

EMG Recording

Per manufacturer guidelines of DataLITE, sensors were placed directly on the muscle belly of the AD, MD, and PM (DataLITE Wireless Sensors & Systems, 2015). Muscle bellies were identified by the participant performing isometric contractions of each of the three muscles. Surface EMG was applied to record the muscle activation patterns using standard surface EMG sensors with a ten-millimeter (mm) contact diameter and a twenty mm spacing between the contacts. EMG sensors were placed bilaterally on the AD, MD, and PM according to the recommendations of the State of the Art on Signal Processing Methods for Surface Electromyography (SENIAM) guidelines (Saeterbakken et al. 2010) and (Schick et al. 2010). For the AD, one sensor was placed on the anterior aspect of the muscle belly, four centimeters (cm) below the clavicle. The MD muscle belly was palpated, and one sensor was placed three cm below the acromion process. A sensor for the PM was placed four cm medial to the axillary fold after palpation for this specific landmark and the muscle belly was performed (Schick et al. 2010).

Statistical Analyses

A Shapiro-Wilk test was utilized in order to determine normality of the data. To assess differences in muscular activation across the three muscles in the six modalities, a repeated measures one-way analysis of variance (RMANOVA) was used in order to compare muscle activation for the normally distributed data. A Friedman ANOVA was utilized for non-normally distributed data. An independent samples t-test was conducted to compare the muscle activity values between males and females. An alpha level of $p \leq 0.05$ was used for all statistical tests, using SPSS version 24.0 software (SPSS, inc., Chicago, IL USA). Cohen's d effect sizes (ES) were also calculated to describe the magnitude of difference between mean scores (<0.2 = trivial, 0.2-0.6 = small, 0.6-1.2 = moderate, 1.2-2.0 = large) (Batterham A.M, Hopkins, W.G 2006).

III. Results

All data for the PM were normally distributed across sessions. The activation of the PM during incline BB (1.55 ± 0.795 mV) compared to decline BB (1.52 ± 0.780 mV) did not display statistically significant differences ($F = 1.039$, $p = 0.737$, $d = 0.127$). The only significant difference observed between PM modalities were during decline DB (1.525 ± 0.618 mV) compared to incline DB (1.4 ± 0.64 mV) ($F=1.060$ $p= 0.011$ $d= 0.159$). All data for the AD were non-normally distributed across sessions and were analyzed using nonparametric tests. A statistically significant difference was observed in the AD activation from an incline position of BB ($F =1.107$. $p= 0.001$ $d= 0.629$) and DB ($F = 1.230$, $p = 0.019$, $d = 0.446$).

All data showed statistically significant differences when comparing the activation of the AD and PM across all modalities ($F \geq 1.55$, $p < 0.006$, $d \geq 2.24$). There were no statistically significant differences for any of the three muscles between flat BB or DB when comparing them within all other modalities ($F \geq 1.212$, $p \geq 0.351$, $d \geq 1.870$) All data for the MD were non-normally distributed across sessions and were analyzed using nonparametric tests.

Significance was observed between MD activity across all conditions ($F \geq 1.15$, $p \leq 0.04$, $d \geq 0.17$) and across conditions in comparison with AD activity ($F \geq 1.58$, $p \leq 0.000$, $d \geq 2.82$), but no significant difference were seen between MD and PM activation ($F \geq 1.28$, $p \geq 0.117$, $d \leq 0.51$).

An independent samples t-test was conducted to compare the muscle activity values between males and females. Significant differences were observed when comparing the PM activation across all modalities ($F \geq 1.68$, $p \leq 0.021$, $d = 1.140$). All AD activation however was not significantly different based on gender ($F \geq 1.58$, $p \geq .177$, $d = 0.740$).

An independent samples t-test was also conducted to compare the biacromial breadth values between males and females. Significant differences were observed when comparing males to females ($F = 4.00$, $p = 0.000$, $d = 13.68$). Male values (38.136 ± 3.22 cm), females (33.1 ± 1.61 cm), totals (35.62 ± 3.58 cm).

Condition			*Muscle*	*Mean (mV)*		*SD*		*Median (mV)*	*p-values*
BB	Incline		PM	1.551	±	0.795		1.525	0.127
			AD	3.412	±	0.882		3.209	0.001
	Flat		PM	1.530	±	0.779		1.526	
			AD	3.145	±	0.944		3.151	
	Decline		PM	1.518	±	0.780		1.532	0.127
			AD	2.839	±	0.928		2.709	0.001
DB	Incline		PM	1.395	±	0.636		1.352	0.011
			AD	2.976	±	1.129		2.493	0.019
	Flat		PM	1.441	±	0.629		1.441	
			AD	2.706	±	0.983		2.550	
	Decline		PM	1.525	±	0.618		1.470	0.011

Table 3. *EMG Recording Results*

IV. Discussion

The purpose of this study was to determine the level of muscular activation of the AD, MD, and PM during different BB bench press and DB press modalities. It was hypothesized that the greatest activation would be observed in the PM during the decline BB press and decline DB press. It was also hypothesized that an inverse relationship would exist between AD activation and PM activation. As expected, a statistically significant difference was observed between the activation of the AD at an incline and decline position of the BB and DB modalities. Differences were also observed between the activation of the PM at an incline and decline position of the DB modality, but no significance was found at an incline and decline of the BB modality.

The effect of DB and BB modalities showed a significant difference between the AD and PM muscle activation, which contrasted with previous findings by Schick (2010). Schick compared the effect of the Smith machine and free weight bench press on the muscle activation of the AD and PM, and Schick's results showed no significant difference between these modalities. The difference between the results of the current study and Schick's may be due to the stability and balance requirements of the shoulder girdle muscles during DB and BB chest press. The free weight bench press offers stability in all three planes of motion (sagittal, frontal, and transverse) forcing the lifter to contract the muscles in a more natural fashion to balance in all three planes of motion while exerting force at a velocity that is not constant (Schick, 2010). When compared to the DB and BB modalities, the Smith machine guides the bar in a fixed path requiring very little balance by the lifter compared with the free weight bench press. Additionally, Schick utilized a grip width of 165% of the individual's biacromial breadth, while our study used 190% of the biacromial breadth. The deviations in biacromial breadth utilized in the two studies may have led to the inconsistent findings. Since our study focused on the DB and BB, the differences among the AD and PM may very well have been due to the variety of stability stipulations required of the DB and BB versus the Smith machine.

Research by Saeterbakken (2011) also contrasts with our findings. Saeterbakken investigated the EMG activity of the AD, PM, triceps brachii, and biceps brachii during BB press, Smith machine bench press, and DB press. The results from Saeterbakken's study showed no differences for the AD and PM among the different exercises, while our research showed significant differences between the AD and PM across all six modalities. The dissimilarities between the current study and Saeterbakken's study could be due to controlling the lifting time during the eccentric and concentric phases of the lifts in Saeterbakken's study. A linear encoder was used to assess the vertical position and lifting time of the DB and BB during all exercises (Saeterbakken, 2011). The repetitions were timed, however they were not completed using a standardized cadance. Along with timed repetitions, dissimilarities between the current study and Saeterbakken's could be due to the differences in grip width placement requirements. Our study utilized a controlled grip width based off subject biacromial breadth, however, Saeterbakken's (2011) methodology allowed subjects to utilize their preferred grip displacement as long as the forefingers were inside the markings on a standard Olympic BB.

An unexpected finding of the current study was the greatest amount of muscle activation within the PM observed at an incline DB and BB rather than a decline position of these modalities. The hypothesis that the greatest activation of the PM would be observed in the decline position not being supported could have occurred due to the differences among direction-specific recruitment. A previous EMG study by Wattanaprakornkul (2011) examined shoulder muscle recruitment patterns during bench press and row machine exercises. To gain a thorough understanding of shoulder muscle coordination during these exercises, a comprehensive investigation of the recruitment patterns of the shoulder muscle groups was required. Significant differences were found in muscle activity levels in all investigated musculature, which included PM, between the bench press and row exercises (Wattanaprakornkul, 2011). The BB press, as well as the DB press, require shoulder movements such as flexion and horizontal adduction, and these movements are direction-specific when performed at incline, flat, and decline positions. Therefore, the greater activation of the PM at an incline position could have been due to the direction-specific recruitment compared to that of the decline position.

The direction of movement in relation to gravity determines the amount of force required to overcome resistive forces. The direction in which a specific muscle or muscle group is capable of exerting force depends on the muscle's relationship or line of pull relative to the joint's axis of rotation. As a joint moves through a particular range of motion, the ability of the line of pull of a particular muscle to change and even result in the muscle having a different or opposite action than in the original position differs based on the muscles involved (Floyd, 2018). With every degree of joint motion, the angle of pull changes as well. Floyd (2018) defines the angle of pull as the angle between the line of pull of the muscle and the bone on which it inserts. When the line of pull for the muscle is

perpendicular to the bone on which it attaches, all of the muscular force is rotary force; therefore, 100% of the force is contributing to the movement (Floyd, 2018). If the angle is less than 90 degrees, the force is a stabilizing force because its pull directs the bone toward the joint axis (Floyd, 2018). If the angle is greater than 90 degrees, the force is dislocating because its pull directs the bone away from the joint axis (Floyd, 2018). The AD, in conjunction with the PM, is an anterior muscle and inserts on the lateral humerus resulting in very similar angles of pull during incline, flat, and decline chest press. The PM displays an angle of pull of 90 degrees during the flat bench press. When the bench is at an incline and decline, however, the angles of pull for this muscle differ. An inclined position gives the PM an angle of pull greater than 90 degrees, and a declined position gives it an angle of pull less than 90 degrees. Consequently, the differences in these angles of pull contribute to variations in force production, which may have contributed to the differences in muscle activation within these modalities.

Furthermore, the PM has two different arrangements of fibers: upper and lower. The upper fibers are located from the medial end of the clavicle to the intertubercular groove of the humerus (Floyd, 2018). The lower fibers are located from the lower ribs and sternum to the intertubercular groove of the humerus (Floyd, 2018). It has been perceived that performing the bench press at the incline position the clavicular head (upper fibers) is targeted while the horizontal position targets the sternocostal head (lower fibers) (Jagessar, Gray, 2010). During a decline chest press, the lower fibers are expected to contribute more to the movement due to the relation of the chest to horizontal. Glass & Armstrong's (1997) data showed no significant difference for upper pectoral activation between the incline and decline bench press. However, there was a significant difference between the incline and decline bench press for the lower sternal portion of the pectoral muscles (Glass, Armstrong, 1997). Because the sensors were not placed directly on the lower fibers of the PM within the current study, the amount of muscle activation recorded could have been less than anticipated during the decline bench press. The lack of support for our hypothesis that the greatest amount of PM activation would be observed in the decline position could have potentially been due to the lack of differentiation of the muscle fiber location during sensor placement.

A study conducted by Paoli (2010) focused on the influence of different ROM (90°, 135°, 185°) at three separate loads (0% 1-RM, 30% 1-RM, 70% 1RM) on selective recruitment of the shoulder muscles in the military press. Paoli conducted this study in order to verify the theory that utilizing an incomplete elbow extension with a reduced ROM would activate only specific muscles (Paoli, 2010). The results showed that the use of the widest ROM increased EMG activity of all the muscles selected with respect to the closest ones (Paoli, 2010). The results also revealed that at the widest ROM the MD resulted in the greatest activation at 70% of the subject's 1RM (Paoli, 2010). Since the greatest amount of activation was seen at 70% 1-RM with the greatest amount of shoulder ROM, the lack of control for this during the present study could have reduced the validity of the results.

When observing the differences in muscle activation across genders, PM across all modalities showed significant differences. However, AD was significantly different between genders only in the flat DB modality ($p = 0.034$). All other AD modalities showed no significant differences. An explanation for these results could be due to the larger amount of subcutaneous adipose tissue in the female chest and its impact on the surface EMG equipment. Surface EMG recordings can be disrupted by any tissue between the sensors and the target muscle. For example, if the target muscle was the piriformis, then the sensor would record interference from all tissues between it and the piriformis. Meaning the EMG sensors would have to penetrate the epithelial tissue, subcutaneous fat, and the gluteus maximus, before the piriformis.

While there were no significant differences in body fat percentage between males and females ($p = 0.599$) there was a large effect size ($d = 1.72$). This large effect size indicates that future research could yield more significant differences if a larger sample size was incorporated. Our study utilized bioelectrical impedance analysis (BIA) as a measure of body composition. BIA measures total body fat, and cannot isolate a specific area of the body such as the chest region. Future research could utilize measurements

that could isolate these specific areas such as skin fold calipers or a dual-energy x-ray absorptiometry.

The research conducted by McCaw and Friday (1994) suggested that shoulder stabilizing muscles were generally more active during free weight bench press compared with a machine bench press, which could have been caused by the greater fatigue in the ancillary muscles (biceps brachii, medial deltoid), attempting to control the free weight bar. McCaw and Friday's study looked specifically at the level of stabilization of the exercise and concluded that an inverse relationship exists between stabilization of the exercise and muscle activation of the stabilizing muscles. McCaw and Friday go on to state that experienced lifters may have developed efficient techniques to control the free weight BB and DBs, thereby reducing the muscle activity in the stabilizing muscles. Thus, a potential limitation of our study could have been in the inclusion of expert lifters, as McCaw and Friday (1994) indicate that expert lifters would have less activation of the stabilizing muscles than novice or beginner level lifters.

V. Practical Application

In this study, three lifts that are consistently used in the development of the AD and PM (incline, flat, and decline) appear to offer different peak muscle activations during two different bench press modes. Since the greatest amount of muscle activation was observed in the PM at an inclined position when comparing across both modes, it can be concluded that DB and BB press in an inclined position is the most beneficial for PM development, particularly the upper fibers, compared to AD and MD. Along with this conclusion is the relation between the AD and PM at both incline and decline positions. The amount of AD activation using DBs in comparison to the BB was observed to be much greater at an inclined than a declined position. For training purposes, this comparison reveals that an incline position is better for targeting AD musculature development. The inference can also be made that the greatest training benefit for the PM is observed using DBs at an inclined position.

References

Clemons, J & Aaron, C. (1997). Effect of Grip Width on the Myoelectric Activity of the Prime Movers in the Bench Press. *The Journal of Strength & Conditioning Research*. 11. 2

Earle, RW. (2006) Weight training exercise prescription. *Essentials of Personal Training Symposium Workbook.* Lincoln, NE: NSCA Certification Commission, 3-39Floyd, R. T. 2018. *Manual of Structural Kinesiology.* New York: McGraw-Hill Education.

Friday, S. & McCaw, J. (1994) A Comparison of Muscle Activity Between a Free Weight and Machine Bench Press, *Journal of Strength and Conditioning Research,* 8, (4).

Glass, S., & Armstrong, T. (1997) Electromyographical Activity of the Pectoralis Muscle During Incline and Decline Bench Press. *Journal of Strength and Conditioning Research,* 11, (3).

Jagessar, M., & Gray, M. (2010). Optimizing Development of the Pectoralis Major. *The Sport Journal,* 13, (1).

Lauver, J. D., Cayot, T. E., & Scheuermann, B. W. (2016). Influence of Bench Angle on Upper Extremity Muscular Activation During Bench Press Exercise. *European Journal of Sport Science,* 16, (3).

Luca, C. J. (1993). Use of the surface EMG signal for performance evaluation of back muscles. *Muscle & Nerve,*16(2), 210-216.

Luca, C. J. (1997). The Use of Surface Electromyography in Biomechanics. *Journal of Applied Biomechanics,*13(2), 135-163.

Newton, R. U., Murphy, A. J., Humphries, B. J., Wilson, G. J., Kraemer, W. J., & HaKkinen, K. (1997). Influence of load and stretch shortening cycle on the kinematics, kinetics and muscle activation that occurs during explosive upper-body movements. *European Journal of Applied Physiology,*75(4), 333-342.

Paoli, A. Marcolin, G. Petrone, N. (2010). Influence of different ranges of motion on selective recruitment of shoulder muscles in the sitting military press: an electromyographic study. *Journal of Strength and Conditioning Research,* 24 (6), 1578-1583.

Saeterbakken, A., Van Den Tillaar, R., & Fimland, M. (2011). A Comparison of Muscle Activity and 1-RM Strength of Three Chest-press Exercises with Different Stability Requirements. *Journal of Sports Sciences, 29,* (5). 533-538

Schick, E., Coburn, J., Brown, L., Judelson, D., Khamoui, A., Tran, T., & Uribe, B. (2010). A Comparison of Muscle Activation Between a Smith Machine and Free Weight Bench Press. *Journal of Strength and Conditioning Research, 24,* (3).

Interpreting Pictures: Bridging the Literacy Gap with Graphic Novels

Daniela Cornelius
Department of English

Abstract – Graphic novels have significantly grown in popularity over the past decade, increasing their impact on modern literary culture. In an effort to engage reluctant readers in literacy education, teachers have utilized graphic novels in their classroom as a bridge to higher forms of literature. The rich illustrations, expressive dialogue, and diversity in topic and voice make graphic novels a viable tool for introducing challenging topics into the classroom. Additionally, educators have looked to graphic novels for their apparent approachability to engage reluctant readers. In this sense, the graphic novel is utilized as a scaffolding tool to higher, text-based forms of literature. While educators often see the added benefits of utilizing graphic novels in the classroom, they continue to prescribe to the notion that the graphic novel is a lower form of literature viable only when used as a scaffold to higher print-based novels that encourage traditional literacy. Looking at graphic novels through this lens is limiting and does not explore their full potential in the classroom. Because graphic novels employ images as well as printed words, they are inherently multimodal texts that educators can utilize as tools for exploring multifaceted forms of literacy. This paper argues for the inherent value in graphic novels as a standalone form of literature that should be utilized within the classroom to reach a growing population of students rooted in a multimodal culture.

I. Introduction

Over the past decade, graphic novels have significantly increased their impact on modern literary culture, securing a place on the shelves of bookstores, libraries, and classrooms. Seen as a popular way to engage readers of all levels, primary and secondary education teachers have looked to graphic novels to introduce challenging topics into their lesson plans. "Many graphic novels offer more diverse voices than traditional textbooks" (Schwarz 62), allowing them to become tools utilized by educators to approach topics such as racism, social inequality, gender bias, and bullying. Art Spiegelman's Pulitzer Prize-winning graphic novel *MAUS: A Survivor's Tale*, for example, encourages readers to consider what it means to have lived during World War II in Nazi-occupied Poland. In the years following its publication, *MAUS* was, and continues to be, featured in many editions of the Norton Anthology of American Literature, earning the distinction as a canonical work of literature. The dichotomy between Spiegelman's life and that of his father, presented in a seamless unification of word and image, validates the potential graphic novels have as a demonstration of complex ideas and emotions, in a popular and widely available format.

Even though graphic novels contain the ability to convey complex lessons, current research trends focus on case studies that introduce graphic novels as a scaffold, or a bridge, to more difficult forms of word-based literature. This type of reasoning only furthers the prevalent notion that graphic novels are a "debased or simplified word-based" form of literature (Jacobs 19). Looking at graphic novels through this lens is limiting and does not explore their full potential in the classroom. Because graphic novels employ images as well as printed words, they are inherently multimodal texts that educators can utilize as tools for exploring multifaceted forms of literacy.

The ubiquitous nature of the internet in our society today has reinforced what Walter Ong anticipated in his 1982 publication, *Orality and Literacy: The Technologizing of the Word*: electronic technology would supplant the hegemonic tradition of print literacy, facilitating a "secondary orality" (133). In the decades since Ong's study, computers, cell phones, and the internet have sustained a

considerable rise in its use and relevance within modernity, cultivating generations of students that increasingly understand their surroundings in a multimodal way. Platforms such as YouTube, Twitter, and Facebook have had an enduring effect on the way text is conveyed and received. In place of the traditional blocks of writing, communication in these social spheres is often truncated, paired alongside videos and images, or altogether replaced by emotive icons. Yet, regardless of the importance of these technological and visual advances in the lives of students, pedagogical standards continue to value written, text-based literacy over its multimodal counterpart. Although educators often see the value of including graphic novels in the classroom as a scaffolding tool to higher forms of literature, the perception that they are a degraded and lower form of literature persists. This paper will seek to argue the inherent value of graphic novels as a standalone form of literature that should be utilized within the classroom to reach a growing population of students rooted in a multimodal culture. The images in graphic novels, in addition to the print, are understood using an exclusive form of visual grammar that allows readers to interpret the images and create meaning based on their social and cultural experiences. Put simply, combining print and images, as in graphic novels, conveys concepts that neither can portray independently; thus, interpreting graphic novels requires a literacy separate from print or visual images (Gee 17-18). This process of interpretation extends the concept of traditional literacy acquired solely from reading text-based books, to include other alternative forms of literacy.

II. History and Reception of Graphic Novels

Comic books and graphic novels have had a long and turbulent history in their reception as a legitimate form of literature. Modern comic books first rose in popularity following the introduction of *Action Comics*, the first superhero comic book, in 1938 (Tychinski). Predominantly appealing to a male audience, comic books continued to surge in the mainstream market as a casual diversion, with "circulation quickly [growing] to an estimated 70 million copies per month in the early 1950s" (Coard qtd in Rice 37). Frederic Wertham's book *Seduction of the Innocent*, in 1954, heightened the growing anxiety that comic books failed to engage their readers in a positive way that promoted literacy. Wertham asserts that "[c]omic books are death on reading" (Jacobs 19) and argues that the inclusion of pictures detracts the reader from focusing on the printed text. According to Wertham, the reader of the comic book exhibits a deterioration in literacy that is attributed to the appeal of the pictures and trivialization of the textual elements of the comic. In response to Wertham's critique and the public outcry that followed, publishers "began to offer a more acceptable, if somewhat bland, type of comic" (Tychinski). While comic books slowly regained the loss of credibility in the early 1980s, the stigma that comic books are a frivolous form of entertainment continues to pervade today.

The graphic novel has followed a similar trajectory in its creation and subsequent reception. Differing in format, the graphic novel is described as "a longer and more artful version of the comic book" (Schwarz 58) often with a single, complex storyline that is followed throughout the entirety of the novel. Although graphic novels have been internationally renowned since the early 20th century, it was not until Marvel Comics published *The Silver Surfer* in 1978 that a graphic novel was widely distributed in the United States. Shortly thereafter, DC Comics published *The Watchmen* and Neil Gaiman's *Sandman*, two of the most popular and best-selling graphic novels of all time. *Spiegelman's MAUS: A Survivor's Tale* is perhaps one of the most world-renowned graphic novels. Following its release, *MAUS* was "nominated for several literary awards, and in 1992 received a special Pulitzer Prize" and has earned the distinction as a canonized work of literature featured in many anthologies. (Tychinski). Today, publishing companies have acknowledged the demand for graphic novels; a wide variety of recreations that range from *Hamlet* to *The Baby-Sitters Club* crowd bookstore shelves alongside original graphic novels like *Brave*, *Persepolis*, and *Fun Home*.

Educators, recognizing their appeal with young readers, have employed graphic novels into their curriculum with great success (see Boerman-Cornell 2016; Carter 2007; Jacobs 2007; Rice 2012; Schmidt 2011; Schwarz 2006). Citing their own personal accounts, instructors claim that

graphic novels help to increase motivation and encourage literacy. William Boerman-Cornell, for example, conducted a study of elementary school students in a reading club to explore the ways in which younger students interact with graphic novels (2016). The results of the study found that students, regardless of their grade, are able to "engage in interpretive activity…showing that graphic novels potentially encourage critical thought in elementary students" (333). Additionally, Boerman-Cornell confirmed that even among the youngest students in the book club, the graphic novel afforded the ability to synergize the elements of the text to derive meaning and form conclusions from the panels. Rather than reading the text and images separately, the study "demonstrated that [participants] could summarize a scene or the larger story to support their argument, interpretation, or observation. Those summaries did not distinguish between information from text and information from images; rather, field notes showed that it seemed to be an unconscious holistic blend of the two modes" (332). Rather than inhibit literacy, as Wertham has once claimed, the amalgamation of text and image encouraged critical-thinking, analysis, meaning-making, and generated discussion among the students in the book club.

Joanna Schmidt similarly employed graphic novels in her first-year college English Skills class to increase the students' interest in their reading materials. Spotlighting graphic novels at the center of each assignment, Schmidt describes the elements of each essay assigned to her remedial composition course. The first essay, a personal narrative about the students' experience with reading, offers an introduction to the course and compels the students to begin interacting with literature. Each assignment represents a new element that is important to the English classroom, increasing in complexity and difficulty. To appeal to reluctant students, Schmidt chose to utilize graphic novels as a scaffolding tool to introduce literary concepts. Over time, Schmidt recognized a transformation in her students' perceptions regarding literature and themselves: "they had thought of themselves as bad readers, but reading something interesting made it easier, more relaxing, and fun. They wrote that by reading a variety of graphic novels, they had come to love them" (106). Although many of the students were first-time readers of graphic novels, the accessible format of the multimodal text afforded them the ability to engage with literature in ways they had never previously considered.

However, despite successes in the classroom, the ways in which graphic novels are applied is problematic. With regard to the maturation of reading and writing literacies in children, "reading comics has almost always been seen as a debased form of word-based literacy, albeit an important intermediate step to more advanced forms of textual literacy, rather than as a complex form of multimodal literacy" (Jacobs 20). As a result, the current educational format continues to uphold Wertham's notion that the graphic novel is a lower form of literature. Literacy pedagogy regards the graphic novel as a scaffold, a way to engage readers through an approachable medium before redirecting them towards more meaningful literature. Reducing the graphic novel to its individual parts, either graphic or textual, rather than treating it as a cohesive, multimodal unit, limits its effectiveness and ability to engage a diverse population of readers already ingrained in a society where images cannot be separated from words. Embracing multimodality "in our teaching at all levels [helps] us to arm students with the critical-literacy skills they need to negotiate diverse systems of meaning making" (21). The graphic novel does not seek to replace traditional forms of literacy; rather, the graphic novel expands orthodox beliefs about literacy by pairing textual and pictorial elements in a way that is accessible by and encompassing of all readers.

III. Evolution of Literacy

Traditionally, the definition of literacy has been limited to the ability to read and write print-based text. Outside of the classroom, however, "[m]essages are now created, inscribed, sent, and received in multimodal ways steeped in the use of new technologies" (Sanders & Albers 1-2). The emergence and subsequent pervasive nature of these technological advancements have increased the need for educators to revise their curriculum to keep students engaged. As such, teachers have looked to multimodal theory as a way to incorporate texts, such as graphic novels, into their classrooms. These

multimodal texts have "expanded the ways [students] acquire information and understand concepts" ("Multimodal Literacies"), requiring a new set of skills that move the student beyond the conventional forms of literacy.

James Paul Gee explains literacy by examining it within the context of primary and secondary discourses. As defined by Gee, a discourse is a "socially accepted association among ways of using language, of thinking, and acting that can be used to identify oneself as a member of a socially meaningful group" (18). In other words, a discourse is comprised of the behaviors and attitudes that allow a person to assimilate within a group. Therefore, family, classroom environments, jobs, and social circles each require a different manner of interaction in order for an individual to operate effectively within that discourse (e.g. an employee would not interact with their supervisor in the same way they would with a friend). Gee emphasizes two different types of discourses: a primary and a secondary. The primary discourse is acquisition of the native language through "face-to-face communication with intimates [family]" (22); secondary discourses consist of social interactions with institutions and people beyond the family that "all build on, and extend, the uses of language we acquired as part of our primary discourse, and they are more or less compatible with the primary discourses of different social groups" (22). Gee contends that the definition of literacy should shift from "the ability to read and write" (21), an ambiguous statement that does not seem to fit within the changing landscape of today's classroom, to "control of secondary uses of language (i.e. uses of language in secondary discourses)" (23). In reframing literacy as a product of discourses, learned social and cultural behaviors are placed at the forefront of literacy, regarded as important devices for meaning-making, rather than inhibitors of knowledge.

Because multimodality has become so prominent in differing aspects of students' lives, we need to consider their discourses inside and outside the classroom. While traditional literacy pedagogy has emphasized reading through learning (defined as a conscious process of gaining knowledge that occurs through formalized instruction), research has shown that students are actually "acquiring these literacies through experiences in the home both before and during school, as well as by the opportunities school gives them to practice what they are acquiring" (Gee 24). Through a process of modeling and trial-and-error, the student is exposed to and gains knowledge of literacy in a natural setting. Unlike learning, acquisition occurs subconsciously and without a prescribed method of teaching (20). The introduction of graphic novels into the classroom provides students with "meta-level cognitive and linguistic skills that they can use to critique various discourses throughout their lives" (24), thereby moving beyond the limited literacy taught by text-based literature. This is not to say that one form of literacy will overtake the other; instead, graphic novels, and similar multimodal texts, offer "multiple forms of representation" that move beyond print (Hassett & Curwood 270), creating a new literacy that incorporates both textual and visual elements. As reading will always occur within the social context of a discourse, the evolution of these discourses will likewise change how students interpret these texts.

IV. Interpretation of the Graphic Novels

Distinct from other genres of literature that include pictures as an illustrated depiction of written text, the images in a graphic novel carry their own meaning that work cohesively with all elements on the printed page. Meaning is obtained from the images using what Kress and van Leeuwen call "visual grammar": "Just as grammars of language describe how words combine in clauses, sentences and texts, so our visual 'grammar' will describe the way in which depicted elements-- people, places, and things-- combine in visual 'statements' of greater or lesser complexity and extension" (1). In a graphic novel, every component on the page is a mode of representation that communicates meaning to the reader. In addition to the literary elements employed within the dialogue and text, readers must also consider the impact the images have on the story. Phillip Wegner, in his consideration of Alan Moore's *The League of Extraordinary Gentlemen*, remarks on the spatial importance of graphic novels, focusing specifically on the negative space between the panels. Quoting Scott McCloud, Wegner writes, "McCloud, in emphasizing the central importance of the third form of spatiality at work in comics, the gutter or

space between the panels, rightly points out, 'it's a mistake to see comics as a mere hybrid of the graphic arts and prose fiction. What happens between these panels is a kind of magic only comics can create'" ('Secondary Literacy,' and the Modernism of the Graphic Novel"). The arrangement of the panels, spacing on the page, font size, typeface, color and shading (or lack thereof), and perspective are all equally important to the reader as they interact with the novel to develop an interpretation of the text. Thus, meaning is achieved through the reader's acuity and use of visual grammar.

Fig 1. *Vladek and Anja walk along a swastika-shaped road. Art Spiegelman, MAUS: A Survivor's Tale, (New York: Pantheon Books, 1986), 125. Print.*

In *MAUS*, for example, the narrator's father, Vladek, describes the desolation he and his wife, Anja, felt when they were unable to find sanctuary from the Nazis invading Poland during World War II. The panel illustrates Vladek and Anja as two mice, an allegorical representation meant to capture simultaneously the Jewish feeling of vulnerability and the anti-Semitic sentiment of perceiving Jewish people as vermin. The mice are walking along a deserted road that is in the shape of a swastika (**see Figure 1**). While the text itself conveys the feeling of helplessness and isolation, the appearance of the swastika emphasizes the reality that any road Vladek and Anja choose will lead to their eventual capture and imprisonment—a message that may have otherwise gone unnoticed without the accompaniment of the image. Additionally, Vladek's speech bubbles order words unusually, relaying through text his non-native English dialect. Meanwhile the visual allegory of mice (and American dogs that saved the mice from the Nazi cats), the swastika-marked lands, the forced perspective that makes Vladek and Anja smaller and posed under the swastika image combine to tell a deeper, richer story than the text alone.

Unlike written grammar, which is learned primarily through formal education, visual grammar is acquired from the experiences and interactions that take place within our social discourses. It is a tool that allows readers "to build a mental picture of reality, to make sense of their experience of what goes on around them and inside them" (Kress & van Leeuwen 2) and yield a meaning that stems from explicit and implicit information gained from culture-specific practices and experiences (3). The reader engages with visual and written grammars to interpret the text: "Such a theory of meaning making with multimodal texts acknowledges the social and semiotic structures that surround us and within which exist, while at the same time it recognizes individual agency and experience in the creation of meaning" (Jacobs 24). Although the author may have an intended interpretation in mind when producing a graphic novel, in his or her absence, the task of deriving meaning from the images and text is placed on the reader, who draws on acquired knowledge from primary and secondary discourses to produce that interpretation (Fish 511). Hence, the product of interpretation is not universal; rather, it is specifically tailored to the relationship a reader has with his or her discourses. Furthermore, in a "dynamically interactive" text, like the graphic novel, "readers (not authors) choose where to look and how to engage with certain aspects of the text" (Hassett & Curwood 271). Therefore, the meaning of each visual element will differ with every reader based on how they interact with their discourses and with the text itself.

In their study of primary education classrooms, Hassett and Curwood observe the ways in which children are able to draw on cultural artifacts and learned social cues to negotiate meaning and attribute an emotional response to pictures in a storybook. Specifically focusing on a page with no written words, the students are asked to consider the different features of the image and make interpretations based on what they see. Pigeon, the main character of the story, "isn't speaking at all, but instead, there is a dark charcoal scribble above his head, his feathers are flying about, and his eyelids are low" (279). When asked to describe how Pigeon

might be feeling, many of the students replied that Pigeon is feeling "angry" and "frustrated" based on his facial expression and "feathers flying all over" (279-280). Despite the lack of printed words, the students are able to interpret the images on the page and assign meaning in a way that contributes to the story. Although the storybook does not explicitly ascribe Pidgeon the feelings of anger and frustration, the children draw from learned social and cultural cues to interpret the images presented to them.

By joining words with images, the graphic novel asks readers to move beyond the hegemonic tradition of the canon that insists on a single, shared understanding, to a consideration of text as a "cultural artifact that readers can use as tools for interpretation and meaning production" (Hassett & Curwood 272). As such, students have a higher stake in the texts introduced in the classroom, enabling them to transition from passive students to active participants of literacy education. In the classroom as a contact zone (see Pratt 1991), the instructor is placed in the role of facilitator between student and text, encouraging students to draw on their primary discourses in a secondary setting.

In their study, Hassett and Curwood show the success of recognizing a visual literacy component of graphic novels; however, their approach continues to regard multimodal literacy as multi-layered, rather than the collective form of literacy discussed by Gee. Still, the students observed by Hassett and Curwood readily identify both reading and writing literacy ideas using their visual literacy, connecting these separate modes as they synthesize and create meaning from images. Regardless of Hassett and Curwood's inability to wholly incorporate multimodality into their study, it does serve to highlight the importance of multimodality in the lives of students. Teaching a multimodal literacy serves a vital function for a digitally literate society, where images and text are continuously aligned with one another. The various elements of the graphic novel, from art style to the font, are meant to foreground the accessibility of this literary genre. The whimsical, yet terrifying, presence of giants in *I Kill Giants*, is meant to captivate its readers while also considering the ways in which we cope with sadness and the terminal illness of a parent; the lack of shading and the central position of Artie and Vladek in *MAUS*, places an importance on the conversational exchange between the two, regardless of what is going on around them; and the uninterested facial expression of Alison Bechdel's father, observed throughout *Fun Home*, demonstrates the dissonance felt by the writer and her father, as they are both forced to suppress their sexuality and perform in socially acceptable ways. Although there is a tendency to equate the approachability of graphic novels with a low form of juvenile literature, the imagery presented within graphic novels embraces an illustrative tradition in literature that expounds a meaning of its own, sometimes in conjunction with the text, and sometimes in spite of it. This same multimodal literacy is perceived in all aspects of our lives, from the junk mail offering to restructure student loan payments, to the internet ad that tries to convince us to click the wrong X on a pop-up window.

V. Looking Ahead

Despite their debased beginnings, graphic novels have grown in popularity in the classroom based on their intriguing and accessible perspective on the literary genre. While there are many case studies that highlight the added benefits of utilizing graphic novels in the classroom, they continue to prescribe to the notion that the graphic novel is a lower form of literature viable only when used as a scaffold to higher print-based novels that encourage traditional literacy. When viewed as a dynamic multimodal text, however, the graphic novel enriches literacy education by adding a visual element that also accounts for the social, cultural, and historical experiences of the reader.

Current evaluation models in education continue to value written literacy over other modes in spite of the prevalence of visual and technological innovations in the lives of students. The use and promotion of multimodal texts like graphic novels are scarce, regardless of their appeal and central role in contemporary society. The need for multimodality in pedagogy is not new, however. In 2005, the National Council of Teachers of Education published a position statement on their website, recognizing the increase in demand for "the intertextuality of communication events that include combinations of

print, speech, images, sounds, movement, music, and animation" ("Multimodal Literacies"). While teachers cannot easily change the infrastructure of the curriculum, they do have the ability to develop a classroom strategy that evolves literacy education to meet the needs of a multimodal generation of students. While it can be a daunting task, several successful case studies, blogs, and book lists exist that can provide educators with the background and resources to successfully transition to a multimodal educational approach.

There is a continued need for further research and case studies examining graphic novels, not as a scaffold, but as its own form of literature. By bridging the gap between traditional and alternative forms of literacy, English pedagogy will benefit from the inclusion of multimodal texts in the curriculum that have the ability to progress traditional literacy by including a visual aspect. As I have previously mentioned, visual literacy does not seek to replace traditional literacy, but rather, enhance it by promoting discourses that are otherwise forgotten when focus is placed solely on text-based literature. The graphic novel grants students the opportunity to explore and acquire multimodality by scaffolding up from their extensive written literacy training in the traditional English and Language Arts classroom to a multimodal literacy. As a result, students shift from passive recipients to active participants that willingly interact with and draw meaning from their texts.

References

Bechdel, Alison. *Fun Home*. Mariner Company, 2007.

Boerman-Cornell, William. "The Intersection of Words and Pictures: Second Through Fourth Graders Read Graphic Novels." *The Reading Teacher,* vol. 70, no. 3, 2016, pp. 327-335.

Carter, Bucky. *Building Literacy Connections with Graphic Novels: Page by Page, Panel by Panel.* National Council of Teachers of English, 2007.

Fish, Stanley. "Response: Interpretation Is Not a Theoretical Issue." *Yale Journal of Law & the Humanities*, vol. 11, no. 2, 1999.

Gainer, Jesse S. and Lapp, Diane. "Remixing Old and New Literacies = Motivated Students." *The English Journal*, vol. 100, no. 1, 2012, pp. 58-64.

Gee, James Paul. "What is Literacy?" *Journal of Education*, vol. 171, no. 1, 1989, pp. 18-25.

Hassett, Dawnene and Curwood, Jen Scott. "Theories and Practices of Multimodal Education: The Instructional Dynamics of Picture Books and Primary Classrooms." *The Reading Teacher,* vol. 63, no. 4, Dec. 2009-Jan. 2010, pp. 270-282.

Jacobs, Dale. "More than Words: Comics as a Means of Teaching Multiple Literacies." *The English Journal,* vol. 96, no. 3, 2007, pp. 19-25.

Kelly, Joe and Ken Jim Niimura. *I Kill Giants*. Bao Publishing, 2018.

Kress, Gunther and Van Leeuwan, Theo. *Reading Images: The Grammar of Visual Design*. 2nd ed., Routledge, 2006.

Lapp, Diane, Moss, Barbara, & Rowsell, Jennifer. "Envisioning New Literacies Through A Lens of Teaching and Learning." *The Reading Teacher*, vol. 65, no. 6, 2012, pp. 367-377.

"Multimodal Literacies." *National Council of Teachers of English*, www2.ncte.org/statement/multimodalliteracies. Accessed 6 March 2018.

Ong, Walter J. *Orality and Literacy: The Technologizing of the Word*. Routledge, 1982.

Pratt, Mary Louise. "Arts of the Contact Zone." *Profession*, vol. 91, 1991, pp. 33-40.

Rice, Mary. "Using Graphic Texts in Secondary Classrooms: A Tale of Endurance." *The English Journal,* vol. 101, no. 5, 2012, pp. 37-43.

Sanders, Jennifer and Albers, Peggy. "Multimodal Literacies: An Introduction." *Literacies, The Arts, and Multimodality*. National Council of Teachers of English, 2010.

Schmidt, Joanna. "Research for the Classroom: Graphic Novels in the Classroom: Curriculum Design, Implementation, and Reflection." Edited by Julie Gorlewski, *The English Journal*, vol. 100, no. 5, 2001, pp. 104-107.

Schwarz, Gretchen. "Expanding Literacies Through Graphic Novels." *The English Journal*, vol. 95, no. 6, 2006, pp. 58-64.

Spiegelman, Art. *MAUS: A Survivor's Tale*. Pantheon, 1986.

Tychinski, Stan. "A Brief History of the Graphic Novel." *The Diamond Bookshelf*, www.diamondbookshelf.com/Home/1/1/20/164?articleID=64513. Accessed 6 March 2018.

Wegner, Phillip E. “Alan Moore, "Secondary Literacy," and the Modernism of the Graphic Novel.” *ImageText*, vol. 5, no. 3, 2010.

Williams, Paul and James Lyons. *The Rise of the American Comics Artist: Creators and Contexts.* University Press of Mississippi, 2010.

Statistical Comparison Between Various Atmospheric Correction Methods and the LibRadtran Package

Christine Evans
Department of Atmospheric Science

Abstract **–** This study investigated the use of LibRadtran to calculate "pixel-size" spectral profiles of the Earth's surface to understand and improve atmospheric corrections of satellite imagery. LibRadtran is a publicly available library of radiative transfer packages used in studies from a variety of scientific fields to compute radiance values, irradiance values, and actinic fluxes in different spectral regions. While widely used as a package for calculating the transfer of radiation within Earth's atmosphere, few studies have compared its results to other atmospheric models more prevalent in remote sensing such as QUick Atmospheric Correction and Dark Object Subtraction. Utilizing the *uvspec* model within LibRadtran, atmospheric profile data from local ozonesonde flights, and satellite measurements from Sentinel-2A and Sentinel-5P TROPOspheric Monitoring Instrument, several spectral profiles were produced for different land types, including forest, concrete, grass and water. Each spectral profile output was plotted in Python to visualize the data before calculating the differences in the three methods. An Analysis of Variance showed that the radiance means of each method vary heavily depending on the land cover type. Concrete and forest varied the most when compared to LibRadtran calculations. These results suggest that the spectral profiles calculated by LibRadtran rely heavily on the albedo profiles specified, which can differ from the "ground-truth." Further investigation into the model's weight on the atmosphere parameters is imperative in determining LibRadtran's effectiveness and accuracy when correcting satellite imagery.

I. Introduction

Background and Purpose

Atmospheric correction is a crucial step in the pre-processing of remotely sensed imagery. This correction adjusts radiance values to reflectance within the imagery, correcting or removing atmospheric effects that could present errors in the image analysis. There are several methods for correcting these effects, including the use of algorithms, correction equations and software programs that have been developed over the years [2]. This study focused on the use of three different methods: QUick Atmospheric Correction (QUAC), Dark Object Subtraction (DOS) and the *uvspec* model within LibRadtran. The objectives were to determine if LibRadtran is an efficient tool to use when atmospherically correcting satellite imagery by producing location specific spectral profiles of different land cover types: grass, forest, concrete, and water and calculate the variance of the LibRadtran-produced spectral profiles between other well-known atmospheric correction methods. The study area focuses on the University of Alabama in Huntsville campus due to the availability of atmosphere data (**Figure 1**).

Radiative Transfer Methods

LibRadtran is a publicly available library of radiative transfer packages that is used for radiative transfer calculations within Earth's atmosphere such as irradiance, radiance, brightness temperature and solar flux. The base of the library evolved from the uvspec radiative transfer model. *Uvspec* calculations take into consideration the radiation coming into the Earth's atmosphere, the atmospheric composition (aerosols, density, pressure, temperature, etc) and cloud cover and have several transfer equation solvers that one can choose from to do the calculations **(Figure 2)** [7].

QUAC is a method of converting in-scene radiance values of satellite imagery to reflectance. It corrects for atmospheric effects without the use of ancillary datasets but by approximating atmospheric conditions based on values already in the image.

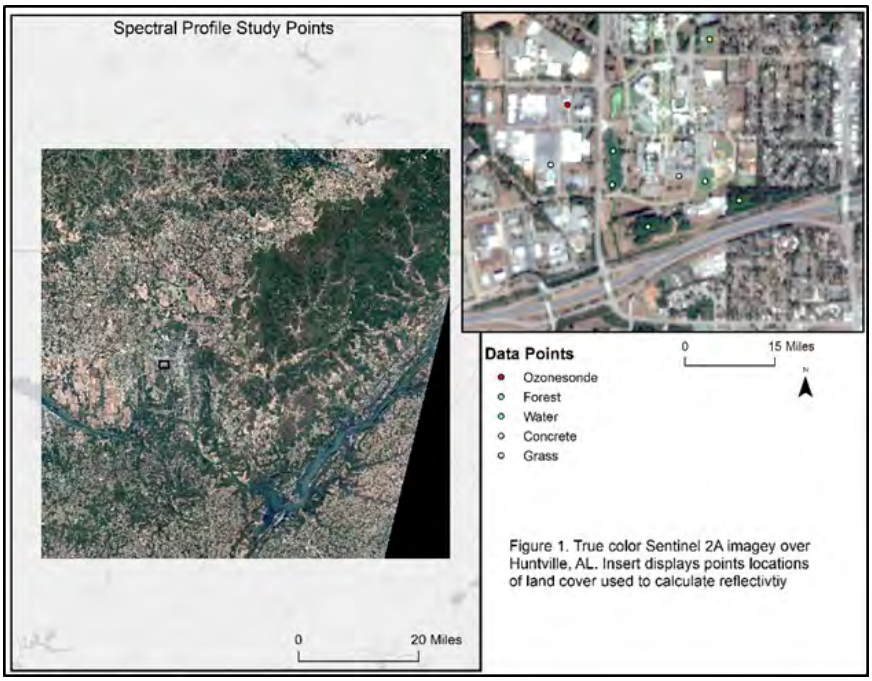

Figure 1. True color Sentinel 2A imagey over Huntville, AL. Insert displays points locations of land cover used to calculate reflectivtiy

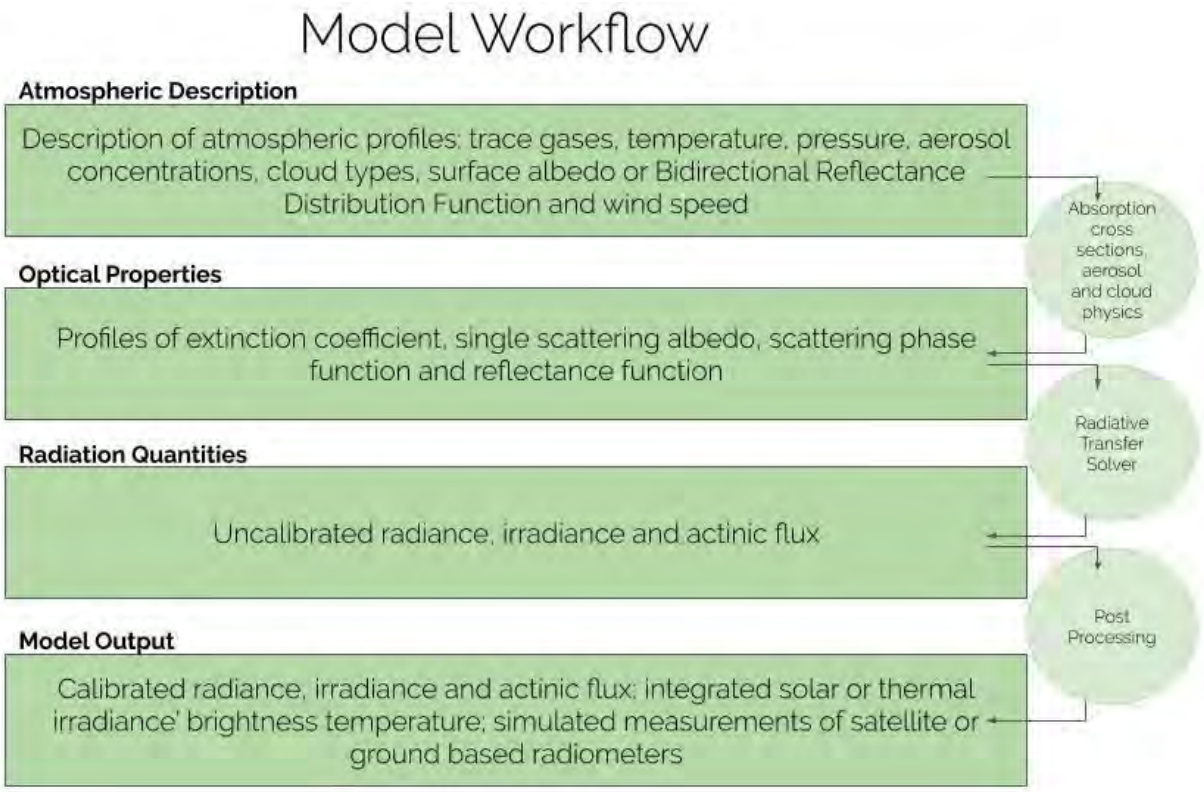

Figure 2. *Uvspec model workflow describing how the model ingests and converts input data.*

QUAC is widely used in remote sensing applications as it produces a reflectance spectrum within 10 percent of ground truth values. This method works best when the imagery being used contains a wide variety of materials such as water, soil, vegetation and man-made materials [4]. DOS is an atmospheric correction tool for satellite imagery that adjusts for atmospheric scattering by subtracting a pixel value chosen to represent the background signature from each band. DOS can be calculated two different ways: band minimum subtraction or region of interest subtraction. Band minimum subtraction uses the minimum DN value of each spectral band for the dark subtraction. DN is the digital number for each pixel of imagery, representing the energy sensed by the satellite. Band minimum subtraction was used for this study [10].

II. Data Methodologies

Data Acquisition

This study utilized several different data sets including measurements from satellite imagery and an ozonesonde launch. Imagery from the Sentinel flight provided land cover data and nitrogen dioxide data and a local ozonesonde launch provided the atmospheric characteristics in profile format. The University of Alabama in Huntsville's Atmospheric Chemistry department launches ozonesondes anywhere from one to three times a month. They provided me the ozonesonde data as comma separated value files describing the atmospheric profiles of the launches. The profiles contain the altitude at which the measurements are taken, pressure, temperature, ozone concentration, ozone column averages, and water vapor. These launches take place on campus and the ozonesonde drift is relatively minimal, providing a good estimate of the atmospheric conditions in Huntsville.

In order to ensure an accurate atmospheric set-up, I needed to make sure the dates of all the data sets aligned as closely as possible, preferably on the same day, this would ensure the atmospheric profile was representative of the land cover image obtained. To do this, I utilized the System's Tool Kit, which is a modeling software that can be used to mimic the timing the movement of objects orbiting the Earth. Given the satellite number and a date range, one can view when a satellite will overpass a specific location on the surface. While providing the dates available for the ozonesonde launches, I was able to determine when the Sentinel 2A and Sentinel-5P satellites would overlap with those dates. Fortunately, all three data sets overlapped on October 5, 2019.

Once I determined overlapping dates, I utilized the Copernicus Open Access Hub to find and download the Sentinel-2A imagery. I utilized the Sentinel Application Platform for resampling and band stacking. For the Sentinel-5P, I utilized Google Earth Engine as the data source. Using already developed code off the Google Earth Engine website, I obtained nitrogen dioxide data from the Sentinel-5P TROPOspheric Monitoring Instrument for the defined points on campus.

Data Progressing

These data sets needed minimum preprocessing before being processed through the three atmospheric corrections methods. Once the Sentinel-2A imagery is re-sampled, bands band 4 (665nm), 3 (493nm), and 2 (560nm) are stacked to create a true color image. This image was first processed through the QUAC capabilities of ENVI **(Figure 3)**. This is a relatively quick process depending on how large the data set is, and the in-scene radiance was converted to reflectively in a matter of minutes. Then the same true color image was processed through the DOS method in ENVI as well, to remove the effects of atmospheric scattering **(Figure 4)**. I compared these new image values to those calculated using the LibRadtran method.

Figure 3. *Images displaying the before and after of processed Sentinel-2A data through QUAC*

Figure 4. *Images displaying the before and after of processed Sentinel-2A data through DOS*

Finally, the data information was processed through the LibRadtran method. While the *uvspec* model within LibRadtran does not ingest a full image, by including the atmospheric characteristics, satellite angles, solar angles, pixel land cover information and radiative transfer information, the model can simulate what the radiance and reflectively of a specific location should be. These simulated reflectivity values are what is being compared to the other two methods. Setting up the *uvspec* input model is relatively easy; the user-manual provides very detailed instructions on how to input the information needed. The first input files contain the atmospheric set up, with reference files containing pressure, temperature, and altitude profiles. From these three inputs, the model calculates air density. The next two lines define the aerosol columns. This is where the ozone and nitrogen dioxide values come in. The next lines define characteristics more specific to the location, such as source of radiation, solar, day of the year in Julian day, albedo profile for the type of land cover within that ”pixel”, solar zenith angle, azimuth angle of the sun, and the latitude and longitude of the location. The final portion defines the specifics needed to calculate radiance or reflectivity. The radiative transfer equation solver I chose to use is the DIScrete ORdinate Radiative Transfer solver (DISORT) which solves **Equation 1**. This solver solves for radiative transfer in 1-D geometry, solving the equation for radiance, irradiance, and actinic flux [2]. The number of streams line is recommended to be set to 16 by the user manual if solving for radiance, so that is done next. Since the true color images are created using band 4, 3, 2; the wavelength range is set to 490 to 665 and set to interpolate the calculation at every 1 whole wavelength. Finally, the output calculation is set to solve for reflectivity, the next input file will calculate for radiance. The next input file adjusts for the solar azimuth angle, cosine of the sensor’s zenith viewing angle and then the sensor’s azimuth angle. Adjusting these settings tells the model to calculate for radiance. **Figure 5 and 6** show example input files.

$$\mu \frac{dI^{dir}(z, \mu_0, \varphi_0)}{\beta^{ext} dz} = I^{dir}(z, \mu_0, \varphi_0)$$

Equation 1. *DISORT solver calculation, where μ_0 and φ_0 are the solar zenith and azimuth angles respectively, z is the radiance at the top of the atmosphere and β^{ext} is optical depth.*

```
                                # Location of atmosphere profile file for Huntsville, AL on October 5 2019
atmosphere_file ...filepath.DAT
mol_modify O3 283. DU       # Set ozone column, data from ozonesonde in Huntsville
mol_modify NO2 0.352 CM_2 # Set NO2 column, data from the Sentinel 5P product
source solar ../data/solar_flux/atlas_plus_modtran
day_of_year 278             # Correct for Earth-Sun distance Julian day (October 5)
albedo_file ...filepath.DAT # Albedo profile of concrete
sza 7.5                     # Solar zenith angle
phi0 284              # Azimuth angle of the sun (0-360)
latitude N 34 [43] [18]       # latitude in deg [min] [sec]
longitude W 86 [38] [49]# latitude in deg [min] [sec]
rte_solver disort     # Radiative transfer equation solver
number_of_streams 16        # Number of streams, default for DISORT radiance
wavelength 490 665          # Wavelength range [B2 - B4nm]
slit_function_file ...filepath.DAT
                            # Location of slit function
spline 490 665 1     #Interpolate from first to last in step
output_quantity reflectivity # Calculate reflectivity

quiet
```

Figure 5. *Example input file to calculate reflectivity in LibRadtran.*

```
include ...filepath #path to above file.

rte_solver disort     # This override what is specified in above file and files included in that file etc.

phi0 148.4            # Solar azimuth angle, set to the solar azimuth angle via image metadata
umu  1                # Output cosine of polar angle (cos4.7 = 0.99), set to the cos(sensor zenith viewing angle)
phi 252.2             # Output azimuth angles, set to sensor azimuth angle of the sensor via image metadata
```

Figure 6. *Example input file to calculate radiance in LibRadtran.*

Data Analysis

Since the output of the LibRadtran method provided radiance, reflectivity had to be calculated by dividing the "uu" column by "edn" column and adjusting the magnitude of the measurement. The "uu" column is the calculated radiance at a specified wavelength and the "edn" column is the diffuse downward irradiance. This division is done to verify the reflectivity calculation done by the first input file. Once the processing through all three methods were completed, the values were plotted using Python to create line graphs displaying wavelength on the x-axis and reflectivity on the y-axis. Line graphs were made for each of the eight-point locations, two of each land cover type. To statistically compare these outputs, a one-way analysis of variance (ANOVA) was computed to determine the variance between the means of the measurements by calculating the f-value and p-value of the datasets. This could only be done for 5 wavelengths, as ENVI only provides the one measurement per band within the wavelength range calculated; therefore, the variance was calculated for those matching wavelengths.

III. Results

Reflexivity Comparison

Each spectral profile produced for the land cover points is plotted to visually determine what the data looks like. Alone they don't tell the viewer much, so they were also plotted together on the same chart to see how the values compare. Looking at **Figure 7** below, the LibRadtran produced value is in green, QUAC in blue and DOS in red.

Analysis of Variance

The ANOVA calculation determined how much the values from one method varied from the other. The greatest variance between group means changed depending on the land cover type. The

f-value provides information on if the means of the datasets were significantly different and the p-value provides whether the null hypothesis should be rejected Comparing QUAC and DOS, the greatest variance is between the concrete groups, QUAC and LibRadtran also is concrete, LibRadtran and DOS is between forest **(Table 1)**. The p-values for the QUAC/DOS and QUAC/LibRadtran are smaller than 0.05, meaning the variance between them is significant.

	QUAC v. DOS		QUAC v. LibRadtran		DOS v. LibRadtran	
	F-value	**P-Value**	**F-value**	**P-Value**	**F-value**	**P-Value**
Grass	0.327	0.578	0.951	0.358	0.064	0.806
Concrete	9.051	0.011	8.432	0.019	0.079	0.785
Forest	0.232	0.639	3.003	0.121	2.371	0.162
Water	2.676	0.128	2.314	0.167	1.875	0.208

Table 1. *ANOVA calculation between the correction methods, using an alpha value of 0.5.*

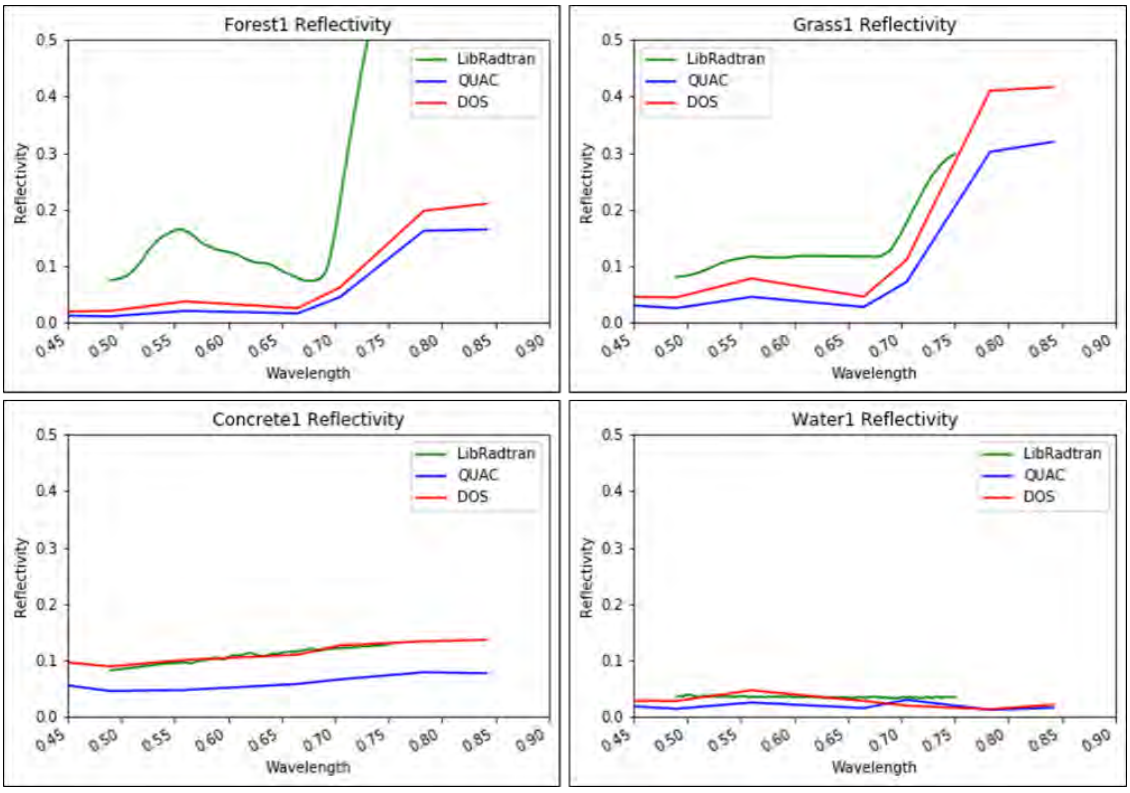

Figure 7. *Plotted reflectivity values for each atmospheric correction method.*

IV. Conclusions

In conclusion, in regard to how simple it is to set up, LibRadtran is fairly easy. While there are not many resources to use online, the user's manual is the best resource. While LibRadtran cannot ingest an image, the calculations can be programmed to loop over several "pixels" if provided the atmospheric setup and albedo profile. The LibRadtran calculated reflectivity resembles the imported albedo profiles. LibRadtran calculated reflectivity was most similar to DOS on the concrete and water surfaces. The shape of profiles on grass and forest followed the in-scene methods closely. With the ANOVA calculations, QUAC/DOS and QUAC/LibRadtran had the greatest variance between concrete means and DOS/LibRadtran had the greatest variance between forest means. These differences may be due to the fact that the in-scene methods (DOS and QUAC) use energy values from within the imagery itself and do not account for atmospheric components surrounding the pixels in question.

V. Discussion and Future Work

This work poses some interesting questions into how much impact the atmospheric set up has on the calculations made by the *uvspec* model. Does the model rely more of the atmospheric conditions or the albedo file used for the land cover type? Future work would investigate this further as well as incorporate a carbon dioxide profile to include the scattering effects of the aerosol. Another project similar to this one could also pose these questions on a more complex atmosphere, possibly a coastal region where there are greater amounts of aerosols in the air. Finally, this work compared LibRadtran, an ancillary data set based calculation, to two different in-scene processes; comparing LibRadtran to processes closer to its set up, MODerate resolution atmospheric TRANsmission or Second Simulation of the Satellite Signal in the Solar Spectrum could pose better results [1].

References

[1] Berk, A., Bernstein, L. S., & Robertson, D. C. (1987). ADA185 384 OTI FILE COPY MODTRAN: A MODERATE RESOLUTION MODEL FOR LOWTRAN.

[2] Buras, R., Dowling, T., and Emde, C.: New secondary-scattering correction in DISORT with increased efficiency for forward scattering, J. Quant. Spectrosc. Radiat. Transfer, 112, 2028 to 2034, 2011.

[3] D. Lu, P. Mausel, E. Brondizio E. Moran (2002) Assessment of atmospheric correction methods for Landsat TM data applicable to Amazon basin LBA research, International Journal of Remote Sensing, 23:13, 2651-2671, DOI: 10.1080/01431160110109642.

[4] ENVI, A. C. M. (2009). QUAC and FLAASH User's Guide. Atmospheric Correction Module Version 4.7, Boulder, CO: ITT Visual Information Solutions.

[5] Guo, Y., Zeng, F. (n.d.). ATMOSPHERIC CORRECTION COMPARISON OF SPOT-5 IMAGE BASED ON MODEL FLAASH AND MODEL QUAC.

[6] Mayer, B, Kylling, A. (2005). Technical note: The libRadtran software package for radiative transfer calculations-description and examples of use. Atmos. Chem. Phys (Vol. 5). Retrieved from www.atmos-chem-phys.org/acp/5/1855/SRef-ID:1680-7324/acp/2005-5-1855EuropeanGeosciencesUnion.

[7] Mayer, Bernhard, Kylling, A., Emde, C., Buras, R., Hamann, U., Gasteiger, J., Richter, B. (2017). Edition for libRadtran version 2.0.2 libRadtran user's guide.

[8] Salman Mahiny, Abdolrassoul Turner, Brian. (2007). A Comparison of Four Common Atmospheric Correction Methods. Photogrammetric Engineering Remote Sensing. 73. 361- 368. 10.14358/PERS.73.4.361.

[9] Song, C., Woodcock, C. E., Seto, K. C., Lenney, M. P., Macomber, S. A. (n.d.). Classification and Change Detection Using Landsat TM Data: When and How to Correct Atmospheric Effects processing step in which correction for atmospheric ef. Retrieved from www.elsevier.com/locate/rse.

[10] Dark Subtraction. (n.d.). Retrieved from https://www.harrisgeospatial.com/docs/AtmosphericCorrection.html.

Utilizing NASA Earth Observations to Assess Coastline Replenishment Initiatives and Shoreline Risk Along Delaware's Coasts

Greta Paris, Rachel Tessier, Ani Matevosian & Nicholas Gagliano
Department of Atmospheric Science

Abstract **–** Delaware's coastline is a vibrant tourist destination and unique habitat for many vulnerable species. Yet, with the lowest mean elevation of any state, this stretch of land is threatened by geological and climatic forces, including coastal erosion, sea level rise, storm surge, and subsidence. The state's Department of Natural Resources and Environmental Control (DNREC) has served as a diligent combatant of coastal land loss since the 1950s. In partnership with the DNREC, this team utilized Landsat 8 Operational Land Imager, Landsat 7 Enhanced Thematic Mapper Plus, Landsat 5 Thematic Mapper, and the Terra Advanced Spaceborne Thermal Emission and Reflection Radiometer in combination with ancillary datasets to create a suite of time-series maps that identified shoreline extent changes in response to management projects and to generate a coastal land loss susceptibility map. Analyses of coastline change across time were performed using quantifiable measures derived from the time-series maps. The team found a statistically significant shift of land to water between 1988 and 2018 ($p < 0.05$). Bombay Wildlife Refuge, Prime Hook Wildlife Refuge, Rehoboth Beach, Slaughter Beach, and Assawoman Bay are the most susceptible areas to land loss along Delaware's coast. Areas that experienced the greatest land loss within the 31-year range were the Prime Hook and Bombay Hook Wildlife Refuges. Conversely, Cape Henlopen exhibited a notable accretion of land. These analyses can be used by the DNREC to support the development of future coastal protection and replenishment strategies through the evaluation of restoration technique effectiveness and identification of at-risk areas.

Keywords:
Delaware, coastline management, erosion, sea level rise, storm surge, subsidence, Landsat, Terra ASTER

I. Introduction

Background Information

Delaware's economically and ecologically vibrant coastline is currently threatened by various climatic and geological forces, including subsidence, coastal erosion, sea level rise, and storm surge. As a popular tourist destination, the coastline fuels the state's economy and it hosts productive fishing, crabbing, and oyster industries (DNREC Public Affairs, 2012). Delaware's coast is also ecologically valuable, as it serves as an important transition zone and migration stopping point for flora and fauna, respectively (DNREC, 2015). For these reasons, the state's government is interested in protecting and restoring the coastline to prevent habitat-loss and property damage.

The state of Delaware lies within the Coastal Plain and has the lowest mean elevation of any state. The Coastal Plain is comprised of unconsolidated soils that are easily erodible (Coastal Hazards in Delaware, n.d.). Research indicates that sea level rise and decreases in sediment supply are the main drivers of shoreline recession (Zhang, Douglas, & Leatherman, 2002). The state also experiences subsidence due to tectonic movement and anthropogenic extraction of subsurface resources, further exacerbating land loss (DNREC, n.d.). Although long-term erosion accounts for the majority of Delaware's coastal land loss (Jesse Hayden, personal communication, September 25, 2019), the state is also impacted by extreme weather events, such as Nor'easters and hurricanes. This is especially true for marshes and wetlands, where average wave conditions, rather than episodic storms, are the dominant cause of marsh boundary loss (Leonardi, Ganju, & Fagherazzi, 2015). An exception to this trend is the break in the natural barrier of Prime Hook

Wildlife Refuge that Hurricane Sandy caused in 2012.

Delaware's Department of Natural Resources and Environmental Control (DNREC) has implemented major shoreline management programs to combat land loss in partnership with the United States Army Corps of Engineers. These programs are generally comprised of beach nourishment and hard structure installation projects and are often funded by the state or federal government (DNREC, n.d.). Research on the effectiveness of beach nourishment in New Jersey during Hurricane Sandy found a slight reduction in damage to beaches that had been nourished since 2000, validating the continuation of these projects (Griffith, Coburn, Peek, & Young, 2015). The most notable restoration project in the area is that of Delaware's Prime Hook Wildlife Refuge, following Hurricane Sandy. This monumental state and federal effort received the 2019 Climate Adaptation Leadership Award for Natural Resources to recognize its innovation and success (Eisenhauer, 2019).

Previous studies demonstrate remote sensing's ability to monitor wetland and coastline changes and restoration efforts (Arcuri, Ortiz, & Edmonds, 2016; Guo, Sheng, Xu, & Wu, 2017; Klemas 2014, Mars & Houseknecht, 2007). For instance, Arcuri et al. (2016) used Landsat imagery of the Mississippi River Delta Plain to identify wind-driven wave edge erosion as a critical driver of the land loss that they quantified. Mars and Houseknecht (2007) also used Landsat imagery to detect a doubling in the erosion rate of a segment of Alaska's coast. A new approach to quantify and map shoreline and coastal wetland water extent is through the use of the Coastal Annual Land Cover Change (CALCC) tool. Created by a previous NASA DEVELOP research team led by Danielle Ruffe, and later modified by a NASA DEVELOP research team led by Christine Fleming, this tool generates synthetic rasters of land and water yearly averages of pixel values.

This project focused on the coastal wetlands and shorelines of Delaware (**Figure 1**) from 1988 to 2018. While Atlantic coastal research is covered by the USGS, the Delaware Bay is left to the state, which has therefore received less research due to budget limitations (Jesse Hayden, personal communication, Oct 1, 2019). Remote sensing data from Landsat 5 Thematic Mapper (TM), Landsat 7 Enhanced Thematic Mapper Plus (ETM+), and Landsat 8 Operational Land Imager (OLI) cover the thirty-one-year period, allowing for an analysis of Delaware's coastline over time via the CALCC tool.

Figure 1. *The study area included a half-mile buffer from Delaware's coastline.*

Project Partners & Objectives

The DNREC has implemented coastal management strategies to tackle the threat of land loss. The DNREC currently does not utilize NASA Earth observations (EOs). The end products developed by the NASA DEVELOP team will enable the DNREC to identify and address coastal areas most in need of intervention to better protect habitats and infrastructure.

This project aimed to support the DNREC in decision-making processes by employing NASA EOs into decision management maps and tools. This has been achieved by exemplifying historical coastline changes in comparison to coastal management programs via several time-series maps and GIFs. Then, the team generated a susceptibility map to highlight areas at-risk to coastal land loss. To quantify possible changes to the coastline, a series of

regressions were performed on the relationships between time and coastal change. The team also created an ArcGIS StoryMap to showcase the unique risks threatening Delaware's coastline, management efforts by the DNREC, and the team's products and results.

II. Methodology

Data Acquisition for Susceptibility Maps

The final susceptibility map is comprised of numerous environmental variables that influence coastal land loss, as shown in **Table 1**. The team chose these factors based on a literature review and the availability of relevant data for use in ArcMap 10.5.1. The team acquired elevation data from a Terra Advanced Spaceborne Thermal Emission and Reflection Radiometer (ASTER) digital elevation model (DEM) and calculated slope from the DEM. We acquired land cover, soil hydrology, and relative sea level rise data from the most relevant, recently available datasets. The team also obtained wind speed and wave height data from the DNREC. Using these data, the team created the coastal land loss susceptibility map.

Table 1. *Data Sources for Susceptibility Factors*

Susceptibility Factors	Data Sources
Elevation	Terra ASTER Digital Elevation Model via NASA Earthdata
Slope	Terra ASTER Digital Elevation Model via NASA Earthdata
Land Cover	National Oceanic and Atmospheric Administration (NOAA) Coastal Change Analysis Program (C-CAP)
Soil Hydrology	USDA/NRCS Gridded Soil Survey Geographic Database (gSSURGO)
Relative Sea Level Rise	NOAA Tides & Currents
Wind Speed	Delaware Environmental Observing System (DEOS)
Wave Height	CB&I Coastal Planning & Engineering, Inc. via DNREC

Data Acquisition for Coastline Change Time-Series Maps & Analyses

To create time-series maps of coastline changes between 1988-2018, the team utilized 5,830 images using three Landsat sensors (**Table 2** and **Figure 2**). Using the CALCC tool, the team acquired and processed these data within the Google Earth Engine JavaScript Application Programming Interface. This processed data was then used within ArcGIS Pro to create time series maps of coastline changes between 1988-2018. One of the time-series maps also showcases the DNREC's historical coastline management projects alongside the coastline changes. Our partners at the DNREC provided us with the historical coastal management project database.

Table 2. *Data Sources for Time-Series Maps and Analyses*

Platform/Sensor	Processing Level	Dataset Type	Number of Images	Dates
Landsat 5 Thematic Mapper (TM)	Collection 1, Tier 1	Surface reflectance	1,699	February 1988 - December 2011
Landsat 7 Enhanced Thematic Mapper Plus (ETM+)	Collection 1, Tier 1	Surface reflectance	1,564	July 1999 - September 2018
Landsat 8 Operational Land Imager (OLI)	Collection 1, Tier 1	Surface reflectance	578	March 2013 - September 2018

Figure 2. *Number of Satellite Images Used Per Year*

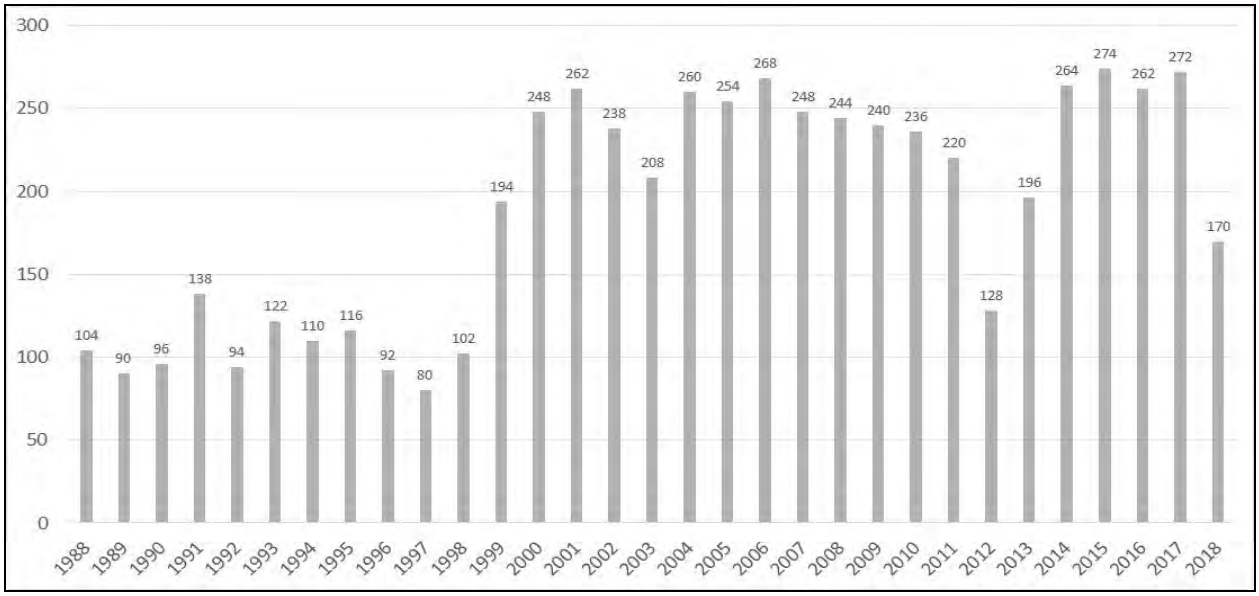

Data Processing for Susceptibility Maps

Elevation

The team classified elevation based on natural breaks in the data. Areas five feet or below are at the greatest risk to erosion, while areas between five and ten feet are at moderate risk. Areas between ten and sixteen feet are at low risk. Finally, areas over sixteen feet are at the least risk.

Slope

The team calculated percent slope from the Terra ASTER DEM using the Slope (Spatial Analyst) tool in ArcMap, then classified the data based on natural breaks. Because Delaware lies in the Atlantic Coastal Plain, the percent slope remained consistently low. Slope was classified based on the following categories: least risk (<1.7%), low risk (1.7%-3.4%), moderate risk (3.4%-6%), and high risk (>6%).

Land Cover

We acquired land cover data from NOAA's C-CAP Land Cover Atlas (Dobson, 1995). Highly developed land, moderately developed land, cultivated cropland, estuarine wetland, unconsolidated shore, and bare land received the classification of the most susceptibility to erosion (National Association of Counties Research Foundation, 1970; Kerris & Iivari, 2006; Titus, 1998). The team classified palustrine wetlands as moderately susceptible (Titus, 1998); lightly developed land, developed open space, and pasture as less susceptible (National Association of Counties Research Foundation, 1970; Kika de la Garza Plant Materials Center, n.d.); and grasslands, deciduous forest, evergreen forest, mixed forest, and scrub/shrub as least susceptible (Kika de la Garza Plant Materials Center, n.d.).

Soil Hydrology

The team acquired the USA Soils Hydrologic Group map layer from ArcGIS Online, with pre-classified soils based on the USDA's Soil Hydrologic Groups A-D. These classifications are characterized by infiltration and runoff rates. Group A has the highest infiltration rate and lowest runoff rate, thus making it the least susceptible to erosion. Group B has a moderately low runoff potential. Group C has a moderately high runoff potential. Group D has the lowest infiltration rate and highest runoff rate, thus making it the most susceptible to erosion (Mockus & Hoeft, 2007).

Relative Sea Level Rise

The team obtained relative sea-level rise (RSLR) data from the NOAA Tides & Currents Database. RSLR includes both sea-level rise and local subsidence rates. The team created Thiessen Polygons within ArcMap to assign RSLR proximity values to the entire coast based on the three measuring stations: Reedy Point, Lewes, and Ocean City (Esri, n.d.).

Wind Speed

The team collected wind speed data from the Delaware Environmental Observing System (DEOS) at six measuring stations along Delaware's coast. The data collected contained a three-year average wind speed for each station. We then reclassified the six measured wind speeds into four groups of susceptibility: very low (4.12-4.38 mph), low (4.38-4.75 mph), moderate (4.75-5.39 mph), and high (5.39-9.46 mph). Lastly, we created Thiessen Polygons in ArcMap to assign wind speed proximity values to the entire coast of Delaware (Esri, n.d.).

Wave Height

We collected wave height data from CB&I Coastal Planning & Engineering, a contractor hired by the DNREC. The team stimulated maximum significant wave height (feet) at five measuring stations based on the Simulating Waves Nearshore Model. Then, the team reclassified the five measured wave heights into four groups of susceptibility: very low (3.6 feet), low (3.7 feet), moderate (3.8 feet), and high (greater than 3.8 feet). Lastly, we created Thiessen Polygons in ArcMap to assign wave height proximity values to the entire coast of Delaware (Esri, n.d.).

Data Processing for Time-series Maps & Analyses

The team used the CALCC tool to process all rasters used in the time-series maps and analyses. This tool masked clouds using the methods of Gorelick et al. (2017), which reassigns cloud-affected pixel to "no data." We omitted interpolation techniques to avoid uncertainty (Length, 2001). To convert the raster imagery to a format that distinguishes between land and water, the CALCC tool uses the Normalized Difference Water Index (NDWI; **Equation 1**) and the Modified Normalized Difference Water Index (MNDWI; **Equation 2**; Jiang et al., 2014). The NDWI equation uses both the green band the near infrared (NIR) band, and the MNDWI equation uses the green band and the mid-infrared (MIR) band. Pixels with a value of zero are classified as land and values of one as water. The pixel values of all rasters for each year are averaged, resulting in a single synthetic raster for each year between 1988 and 2018 in a Georeferenced Tagged Image File Format. Pixels with values between zero and one represent locations that changed for that year. The raster calculator within ArcGIS Pro enabled the quantification of year-to-year change, by using **Equation 3**.

(1) $NDWI = \frac{GREEN - NIR}{GREEN + NIR}$

(2) $MNDWI = \frac{GREEN - MIR}{GREEN + MIR}$

(3) $Change = Year_{Final} - Year_{Initial}$

Data Analysis for Susceptibility Maps

The team performed a weighted sum of slope, land cover, and soil hydrology to create the susceptibility to erosion map (Esri, n.d.), where each factor had a weight of 1.00. The team then reclassified the susceptibility to erosion map into four classes based on equal intervals. A spectrum of red to green represents areas from most to least susceptibility, respectively.

The team performed a second weighted sum of elevation, susceptibility to erosion, wind speed, wave height, and relative sea-level rise to create the overall coastal land loss susceptibility map (Esri, n.d.). We assigned a weight of 1.00 to elevation and susceptibility to erosion, a weight of 0.50 to wind speed and wave height, and a weight of 0.75 to relative sea-level rise. We then reclassified this map into four classes based on natural breaks, again with a spectrum of red to green that indicates high to low susceptibility.

Data Analysis for Time-Series Maps & Analyses

Using the GEE Javascript API, the CALCC tool yielded a classification of land and water pixels within our study area. This allowed for the analysis and quantification of land loss and accretion over the thirty-one-year period, as well as the rate of that change, which was calculated with the Raster Calculator (Spatial Analyst) Tool within ArcGIS Pro (Esri, n.d.; **Equation 3**). Within Microsoft Excel, we regressed both the annual averages and year-to-year changes to detect potential trends in land change and land change rates through time. More specifically, we performed linear and quadratic regressions, with alpha values below 0.05 being deemed significant. The team then created three GIFs within Adobe Premiere Pro for qualitative analyses, including the coastline changes for the entire study area through time with the beach management projects, shoreline changes for the Prime Hook Wildlife Refuge and Cape Henlopen area, and the Bombay Hook Wildlife Refuge.

III. Results & Discussion

Susceptibility Maps

The coastal land loss susceptibility map **(Figure 3)** encompasses the entire coast of Delaware and all susceptibility factors. The team obtained the datasets for each susceptibility factor from government sources, such as NOAA, USDA, and DNREC, some of which were dated. Additionally, wind speed and wave height data do not extend into the tidal wetlands found on Delaware's Atlantic coast. With dates and areas differing for each dataset, the team found it difficult to sum the factors with mathematical precision (see section 3.3). A map displaying susceptibility to erosion, exclusively, is comprised of the slope, land cover, and soil hydrology factors. This susceptibility to erosion map, along with the maps of every susceptibility factor, can be found in the Appendix.

Areas of high susceptibility to land loss tended to have vulnerable land cover and soil hydrology. These areas include Bombay Hook Wildlife Refuge, Prime Hook Wildlife Refuge, Slaughter Beach, Rehoboth Beach, and Assawoman Bay. Assawoman Bay is particularly susceptible due primarily to high rates of relative sea level rise. Areas of low susceptibility showed characteristics of having adequate land cover and soil hydrology. Furthermore, these areas were the least affected by relative sea level rise, wind speed, and wave height and were comprised of the western portion of Rehoboth Bay and most of the coastline north of Bombay Hook.

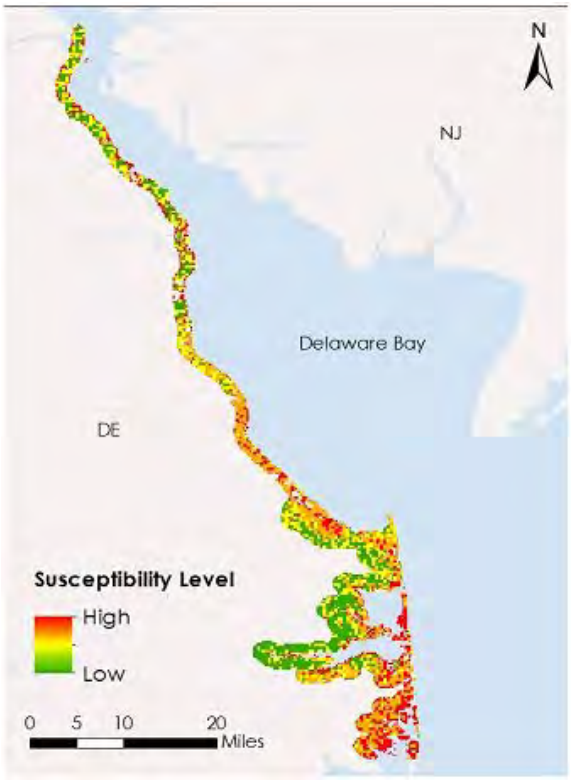

Figure 3. *Coastal land loss susceptibility of Delaware's coast.*

Time-series Maps & Analyses

The time-series map of the entire study area and historical management projects lacks certain project-specific information, though it was informative in showing changes in percent water. However, the team detected trends in overall land loss, both qualitatively and quantitatively. **Figure 4** encompasses the coastal change for the entire study area as well as the changes for two areas of interest. As can be seen, Bombay Hook Wildlife Refuge experienced considerable land loss over the thirty-one-year period due primarily to chronic erosion. The Little Creek Wildlife Area experienced coastal loss but also exhibited land accretion within its inland portions. Kitts Hummock exhibited coastal and inland land loss. Prime Hook Wildlife Refuge exhibited the most dramatic changes. Up to 2012, the loss and accretion of this area appeared to be largely cyclical. The break in the natural barrier of this refuge by Hurricane Sandy in 2012 is evident within our time-series maps, as well as the extensive restoration efforts of state and federal entities. An important temporal landmark can also be found within these maps. In 1995, the construction of the Wolfe Neck Wastewater Treatment Facility occurred and is visible within these maps. The representation of its ponds serves as an assurance of the validity of the CALCC tool.

Another notable implication of the land change map of **Figure 4** is that of the Bombay Hook Wildlife Refuge. Apart from the fact that the area has experienced considerable land loss, it is clear via our partner-provided beach management project dataset that this area has never received land loss intervention projects by state or federal entities. The loss of this area must be primarily due to chronic erosion, as the visual rate of loss evident in the GIFs is gradual. Chronic erosion is the geologic force of land loss that our partners are most interested in, and it is likely that they will find this information invaluable moving forward in their decision-making processes.

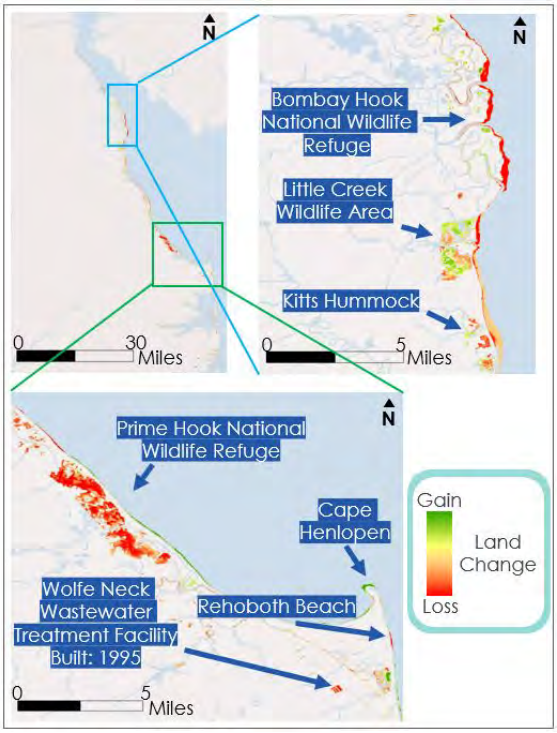

Figure 4. *Maps of coastal land loss between 1988 and 2018 (see **Equation 3**). Map A showcases the change of the entire study area. Map B encompasses an area of interest, from Bombay Hook Wildlife Refuge south to Kitts Hummock. Map C encompasses the second area of interest that includes Prime Hook National Wildlife Refuge, Cape Henlopen, Rehoboth Beach, and the Wolfe Neck Wastewater Treatment Facility.*

The change in percent water through the years is plotted in **Figure 5**, and the rate of that change is exhibited in **Figure 6**. Notable events are reflected within the respective years of these plots. For instance, Hurricane Sandy and the subsequent inundation of Prime Hook Wildlife Refuge is reflected in the considerable increase in water between 2012 and 2013. And the marsh restoration projects that began in 2015 can also be seen in these plots by the decrease in water, or increased rate of land accretion.

A quadratic regression had a better fit for both plots than linear regressions (quadratic fit for **Figure 5**: $R^2 = 0.7611$; linear fit for **Figure 5**: $R^2 = 0.7534$; quadratic fit for **Figure 6**: $R^2 = 0.0061$; linear fit for **Figure 6**: $R^2 = 0.0041$). Both the negative quadratic and a significantly positive linear trend (p-value= 2.55699E-10) for **Figure 5** suggest a thirty-one-year trend of coastal land loss, rather than accretion. The regressions for **Figure 6** are largely inconclusive. The inconclusiveness in the regressions for **Figure 6** stems from the cyclical nature of the change from land to water, thus causing the curve to cycle up and down over the zero line. The change in time over the years does not have much of a relationship to the change from land to water, resulting in a low R^2 value.

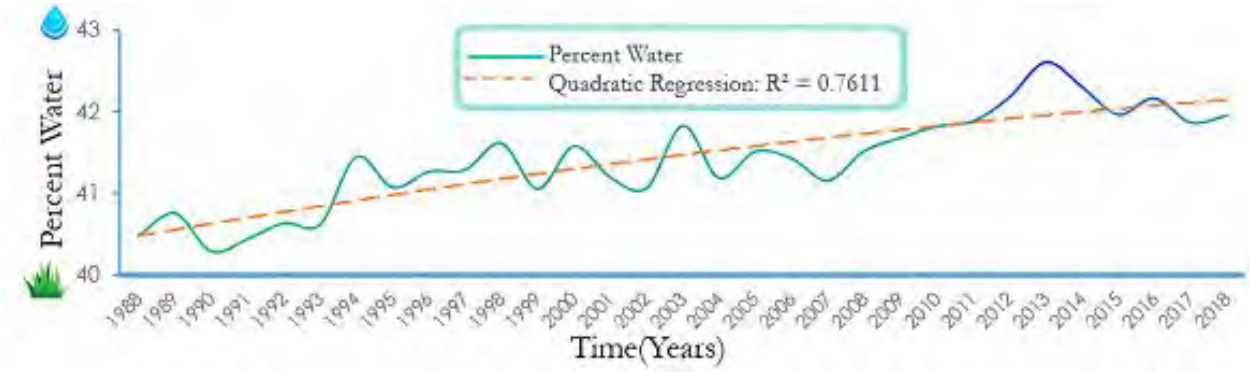

Figure 5. *Coastal land change of Delaware's coast from 1988 to 2018.*

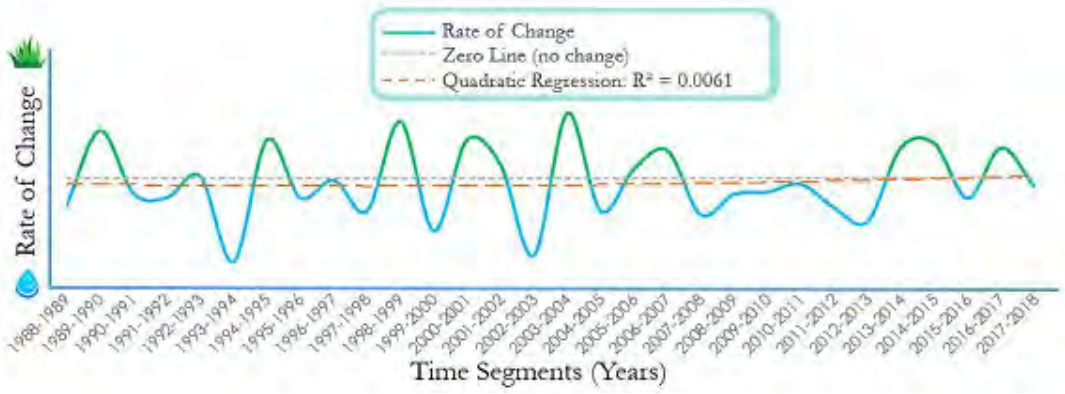

Figure 6. *Rate of Delaware's coastal land change from 1988 to 2018. The y-axis units are represented by a water droplet icon and a grass icon that represent the change to land or water above the Zero Line that represents no change.*

Future Work

There are three key areas that should be addressed moving forward. Little research has been done regarding Delaware's vulnerability to subsidence-caused land loss, and the inclusion of subsidence via relative sea level rise is what makes our susceptibility map novel. The additional use of the Sentinel-1 interferometric synthetic aperture radar (InSAR) instrument can provide our partners with an even more informative time-series map of the state's vertical mobility, namely subsidence, as well as higher quality mapping overall, particularly for the factors of elevation and slope (ESA, 2019). The socioeconomic distinction between the two stretches of Delaware's coastline are quantifiable, as residents near the Bay's coastline are socially more vulnerable to environmental threats according to the Centers for Disease Control (CDC, 2018). It would be interesting and informative to incorporate the social vulnerability factors from this federal entity with the susceptibility information that our team has developed to discern which communities are truly the most vulnerable. And finally, our results are not validated, which is a limitation that can be remedied through the use of our partner's substantial reserves of in situ datasets.

IV. Conclusions

As demonstrated within this project, the DNREC and organizations like it can utilize NASA's EOs to explore historical, current, and potential spatial phenomena. The team has shown both qualitatively and quantifiably that Delaware's coast has experienced land loss since 1988 but found no detected trend in the rate of land change. Prime Hook and Bombay Hook National Wildlife Refuges, Slaughter Beach, Rehoboth Beach, and Assawoman Bay are the most susceptible areas to land loss along Delaware's coast. The Prime Hook and Bombay Hook National Wildlife Refuges have experienced the greatest amount of land loss from 1988-2018. Three interesting occurrences detected by the Landsat satellites exhibited the break in the natural barrier of the Prime Hook Wildlife National Refuge by Hurricane Sandy, the subsequent marsh restoration, the chronic erosion of Bombay Hook National Wildlife Refuge, and the construction of a wastewater treatment facility. Although limitations existed within the coastal management project's information, supporting evidence showed that the Bombay Hook Wildlife Refuge, the area that experienced the most extreme chronic erosion, has never received federal or state intervention. This illuminating notion is just one example of an instance in which these products can help the DNREC in their decision-making processes moving forward.

V. Acknowledgments

Our NASA DEVELOP research team would like to thank our partners at the Delaware DNREC, Jesse Hayden, Ashley Norton, Joe Faries, and Sierra Davis. Thank you, also, for the support from our science advisors, Dr. Jeffrey Luvall and Dr. Robert Griffin. And of course, we are grateful for all the guidance from our mentors and colleagues, Danielle Ruffe, Maggi Klug, Helen Baldwin, Christine Evans, and Madison Murphy.

Any opinions, findings, and conclusions or recommendations expressed in this material are those of the author(s) and do not necessarily reflect the views of the National Aeronautics and Space Administration.

This material is based upon work supported by NASA through contract NNL16AA05C.

References

[1] Arcuri, J. L., Ortiz, A. C., & Edmonds, D. A. (2016). Remote Sensing Analysis of Land Loss Processes in the Mississippi River Deltaic Plain. Geological Society of America Abstracts with Programs, 48(7). doi: 10.1130/abs/2016AM-286113.

[2] CB&I Coastal Planning & Engineering, Inc. (2015). State of Delaware Bay Beach Design Verification Report. State of Delaware Bay Beach Design Verification Report (pp. 1–125).

[3] CDC's Social Vulnerability Index (SVI). (n.d.). Retrieved November 19, 2019, from https://svi.cdc.gov/map.html

[4] CERES Science Team. (2015). CERES Level 3 SYN1DEGDAYTerra+Aqua netCDF file, Edition 3A. NASA Atmospheric Science Data Center, accessed 11 February 2016. doi://10.5067/Terra+Aqua/CERES/SYN1degDAY_L3.003A

[5] Copernicus Sentinel-1 Supports Detection of Shoreline Positions. (2019, May). Retrieved from https://sentinel.esa.int/web/sentinel/news/-/article/copernicus-sentinel-1-supports-detection-of-shoreline-positions

[6] Delaware Department of Natural Resources and Environmental Control. (n.d.). A Line in the Sand: Beach Preservation. Retrieved from https://perspectives.dnrec.delaware.gov/stories/s/A-Line-in-the-Sand-Beach-Preservation/3aqi-49z2/

[7] Delaware Department of Natural Resources and Environmental Control. (2015). Chapter 2: Delaware's Wildlife Habitats. 2015 Delaware Wildlife Action Plan. Retrieved from http://www.dnrec.delaware.gov/fw/dwap/Pages/default.aspx

[8] Delaware Environmental Observing System. (2019). Retrieved from http://www.deos.udel.edu/

[9] DNREC (n.d.). Coastal Hazards in Delaware. [PowerPoint slides]. Retrieved from: http://www.dnrec.delaware.gov/swc/Shoreline/Documents/Coastal%20Resiliency/coastal_hazards_overview.pdf

[10] DNREC Public Affairs (29 May 2012). Delaware Bayshore Initiative Launched to Spur Conservation, Recreation, and Eco-Tourism in State's Coastal Communities. [Press release]. Retrieved October 7, 2019, from http://www.dnrec.delaware.gov/News/Pages/Delaware-Bayshore-Initiative-given-national-launch-to-spur-conservation,-recreation-and-eco-tourism-within-state.aspx

[11] DNREC (n.d.). Sea Level Rise and Delaware's Wetlands. Retrieved from http://www.dnrec.delaware.gov/Admin/DelawareWetlands/Pages/Sea-Level-Rise.aspx

[12] DNREC (n.d.). Topic: Wetlands. Retrieved from https://dnrec.alpha.delaware.gov/wetlands/

[13] Dobson, J. (1995, April). NOAA Coastal Change Analysis Program: Guidance for Regional Implementation. Retrieved October 16, 2019, from https://coast.noaa.gov/digitalcoast/training/ccap-land-cover-classifications.html

[14] Eisenhauer, D. (2019, September 23). Prime Hook National Wildlife Refuge marsh restoration effort recognized as a national model for climate adaptation leadership. Retrieved November 19, 2019, from https://www.fws.gov/news/ShowNews.cfm?ref=prime-hook-national-wildlife-refuge-marsh-restoration-effort--recognized-&_ID=36464

[15] Esri. (n.d.). Create Thiessen Polygons. Retrieved November 5, 2019, from https://pro.arcgis.com/en/pro-app/tool-reference/analysis/create-thiessen-polygons.htm

[16] Esri. (n.d.). Weighted Sum. Retrieved October 17, 2019, from http://desktop.arcgis.com/en/arcmap/10.5/tools/spatial-analyst-toolbox

[17] Gorelick, N., Hancher, M., Dixon, M., Ilyushchenko, S., Thau, D., & Moore, R. (2017). Google Earth Engine: Planetary-scale geospatial analysis for everyone. Remote Sensing of Environment.

[18] Griffith, D. A., Coburn, S. A., Peek, K.M., & Young, R. (2014). Hurricane Sandy: Did Beach Nourishment Save New Jersey? Learning from the Impacts of Superstorm Sandy (pp. 57-67). Academic Press.

[19] Guo, M., Li, J., Sheng, C., Xu, J., & Wu, L. (2017, April 5). A Review of Wetland Remote Sensing. Retrieved from https://www.ncbi.nlm.nih.gov/pmc/articles/PMC5422050/

[20] Houseknecht, D. W., & Mars, J. C. (2007, July 1). Quantitative remote sensing study indicates doubling of coastal erosion rate in past 50 yr along a segment of the Arctic coast of Alaska. Retrieved from https://pubs.geoscienceworld.org/gsa/geology/article-abstract/35/7/583/129876

[21] Interferometry. (n.d.). Retrieved from https://sentinel.esa.int/web/sentinel/user-guides/sentinel-1-sar/product-overview/interferometry

[22] Jiang, H., Feng, M., Zhu, Y., Lu, N., Huang, J., & Xiao, T. (2014). An automated method for extracting rivers and lakes from Landsat imagery. Journal of Remote Sensing, 6, 5067-5089; doi: 10.3390/es6065067

[23] Kerris, C. A., & Iivari, T. A. (2006, April 2). Soil Erosion on Cropland in the United States: Status and Trends for 1982-2003. Retrieved October 30, 2019, from https://pdfs.semanticscholar.org/9b26/6deec84089b01e201057b7f6fbf73feedcff.pdf

[24] Kika de La Garza Plant Materials Center. (n.d.). Vegetative Barriers for Erosion Control. Retrieved October 30, 2019, from https://www.nrcs.usda.gov

[25] Klemas, V. "Remote Sensing of Riparian and Wetland Buffers: An Overview," Journal of Coastal Research 30(5), 869-880, (1 September 2014). https://doi.org/10.2112/JCOASTRES-D-14-00013.1

[26]Landsat Level 3 Dynamic Surface Water Extent (DSWE) Science Products courtesy of the U.S. Geological Survey.

[27] Lenth, R. (2001). Some practical guidelines for effective sample size determination. The American Statistician, 55(3), 187-193. Retrieved from http://www.jstor.org/stable/2685797

[28] Leonardi, N., Ganju, N. K., & Fagherazzi, S. (2016). A linear relationship between wave power and erosion determines salt-marsh resilience to violent storms and hurricanes. Proceedings of the National Academy of Sciences, 113(1), 64–68. https://doi.org/10.1073/pnas.1510095112

[29] Mockus, V., & Hoeft, C. C. (2007, May). Hydrologic Soil Groups. Retrieved October 8, 2019, from https://directives.sc.egov.usda.gov/OpenNonWebContent.aspx?content=17757.wba

[30] NASA/METI/AIST/Japan Spacesystems, and U.S./Japan ASTER Science Team (2019). ASTER Global Digital Elevation Model V003 [Data set]. NASA EOSDIS Land Processes DAAC. Accessed 2019-11-19 from https://doi.org/10.5067/ASTER/ASTGTM.003

[31] National Association of Counties Research Foundation. (1970, May). Urban Soil Erosion and Sediment Control. Retrieved October 30, 2019, from https://nepis.epa.gov

[32] NOAA Sea Level Rise Viewer. (2019, July). Retrieved from https://coast.noaa.gov/slr/#/layer/vul-soc/0/-8412188.727325013/4737691.101190568/9/satellite/none/0.8/2050/interHigh/midAccretion

[33] Sea Level Trends. (2018). Retrieved from https://tidesandcurrents.noaa.gov/sltrends/sltrends.html

[34] Shoreline and Waterway Management Section. (n.d.). Retrieved September 27, 2019, from http://www.dnrec.delaware.gov/swc/Shoreline/Pages/Shoreline.aspx

[35] Titus, J. G. (1998). Rising Seas, Coastal Erosion, and the Takings Clause: How to Save Wetlands and Beaches Without Hurting Property Owners. Retrieved October 31, 2019, from http://digitalcommons.law.umaryland.edu

[36] The Delaware Geological Survey. (n.d.). Retrieved from https://www.dgs.udel.edu/delaware-geology/summary-geologic-history-delaware

[37] USA Soils Hydrologic Group. (2019, June). Retrieved from https://landscape11.arcgis.com/arcgis/rest/services/USA_Soils_Hydrologic_Group/ImageServe

[38] U.S. Census Bureau (n.d.). Small Area Income and Poverty Estimates (SAIPE). Retrieved October 7, 2019, from https://www.census.gov/data-tools/demo/saipe/#/expandedMap?map_geoSelector=mhi_c&s_measures=mhi_snc&s_year=2017&s_state=10

[39] U.S. Department of Commerce, N. N. C. for E. I. (n.d.) NOAA Marine Environmental Buoy Database. Retrieved September 30, 2019, from https://www.nodc.noaa.gov/BUOY/

[40] U.S. Geological Survey Earth Resources Observations and Science Center. (2018). Landsat ETM+ Level-1 Surface Reflectance (SR). Science Product. U.S. Geological Survey. https://doi.org/10.5066/F7WH2P8G

[41] U.S. Geological Survey Earth Resources Observation and Science Center. (2012). Landsat TM Level-2 Surface Reflectance (SR) Science Product. U.S. Geological Survey. https://doi.org/10.5066/f7kd1vz9

[42] U.S. Geological Survey Earth Resources Observations and Science Center. (2018). Landsat OLI Level-1 Surface Reflectance (SR). Science Product. U.S. Geological Survey. https://doi.org/10.5066/F71835S6

[43] Zhang, K., Douglas, B., & Leatherman, S. (2002). Do Storms Cause Long‐Term Beach Erosion along the U.S. East Barrier Coast? The Journal of Geology, 110(4), 493–502. https://doi.org/10.1086/340633

Differences in Player Metrics Between Lacrosse Games and Practices

Kinta Schott
Department of Kinesiology

Abstract **–** This study was intended to better understand the physiological demands of the sport of lacrosse by analyzing and comparing player metrics during game and practice sessions. A team heart rate monitoring system with global positioning was utilized to measure player metrics during games, which were compared with metrics recorded during practice sessions. Participants in the study consisted of 13 male high school club lacrosse players (16.2 ± 1.5 yr; 175.3 ± 7.7 cm; 69.9 ± 13.6 kg). Game and practice data were compared utilizing paired samples *t*-tests, while individual position metrics were analyzed by independent samples *t*-tests. A standard $p \leq .05$ and effect size (r) were used to determine significance and effect sizes. Results of game and practice comparison showed significant differences for average HR, total calories, and caloric expenditure *(*$t \geq 4.2$, $p \leq .003$, $r \geq .590$). Significant differences were also found for duration, total distance covered, and number of sprints performed between game and practice sessions ($t \geq 2.32$, $p \leq .049$, $r \geq .253$). Positional comparisons identified significant differences and large effect sizes between midfield and face off positions for maximum HR ($t=2.411$, $p=.028$, $r=.525$) and number of sprints ($t = 3.242$, $p = .005$, $r = .745$). Games showed lower total caloric expenditure, but duration of the sessions was significantly different. When session duration was normalized, players showed a higher caloric expenditure during games. As a result of these findings coaches may want to change their practice session intensities if they wish to emulate games.

Keywords: positional differences, heart rate monitor, global positioning, physiological outputs, field athletes

I. Introduction

There were 324,689 lacrosse players in the United States in 2017 according to US Lacrosse's "2017 Participation Survey". The sport of lacrosse has been one of the fastest growing sports in the US with boy's programs increasing participation by 24 percent between 2012 and 2017. Lacrosse has been dubbed the "fastest sport on two feet" ("Making the Fastest Game on Two Feet Faster," 2016) and it has a growth rate to match. The rise of participation in lacrosse has also led to an increase in research of the physiological demands of the sport. Current research, has been focused toward laboratory-based testing on lacrosse players, utilizing common maximal effort tests such as one repetition max, the Bruce Protocol (Enemark-Miller, Seegmiller, & Rana, 2009), and the Wingate test (Steinhagen, Meyers, Erickson, Noble, & Richardson, 1998). However, there is limited real-time data collected in field-based settings. Although laboratory methods are ideal for testing peak performance, they may not be accurate in predicting the actual demand of lacrosse players during competition. Research has been done comparing laboratory performance tests and in game measures for other sports and has shown discrepancies between laboratory measurements and actual playing abilities and player metrics in competitive events. Results from a study conducted by Bond, Bennett, and Noonan (2018) concentrated on hockey athletes and showed that the data resulting from the use of laboratory and functional movement tests are inconsistent and suggest that they may not reveal information about a player's sport-specific skill or capability. Additionally, research on other sports has shown insight into player conditioning levels and the need for data following live play to understand the physiological requirements of athletes in their respective sports. Soccer, a widely studied sport, is very similar to lacrosse in the individual positions and playing surfaces. During game play,

soccer players reach average heart rates of 70-85% of their maximum rate (HR max), they can spend 8.1-8.7 percent of their game in a high intensity run or sprint, and they cover an average of 10.8 km per match (Sapp et al., 2017). Because these demands have been studied for more than five decades, the research is able to provide the average distance covered and athlete's average intensity as a percentage of maximal heart rate. Without real-time data collection during competition, it is difficult to elucidate the true performance demands existing in the sport of lacrosse. The use of data found during game situations for lacrosse players may help to better understand the true demands during game play. The opportunity to study lacrosse players in similar ways exists and is necessary to better understand the physiological and conditioning requirements for the players participating in this rapidly growing sport.

The sport of lacrosse is a team sport with four primary positions: attack, midfield, defense, and goalie. Each position has its own responsibilities and physiological requirements. Traditionally, the midfield covers the entire field, end to end, while the attackers and defenders cover their respective ends. The goalie guards the goal often with minimal movement. In the men's game, there is also a specialized position, called a face off get off (FOGO). A FOGO begins play at the start of the game and after every goal. Men's lacrosse is typically played on a natural grass or synthetic turf field. The dimensions for the field are 110 yards long by 60 yards wide. The mid-line of the field is also referred to as the restraining line which is to prevent defenders from going onto the attacking area and attackers from entering the defensive end. Midfielders, however, are free to roam end to end, provided no more than six total field players from each team are on the side of play (Smith, 2017). Goals are placed 80 yards apart to provide 15 yards behind the goal line extended for play (Scroggs, 2018).

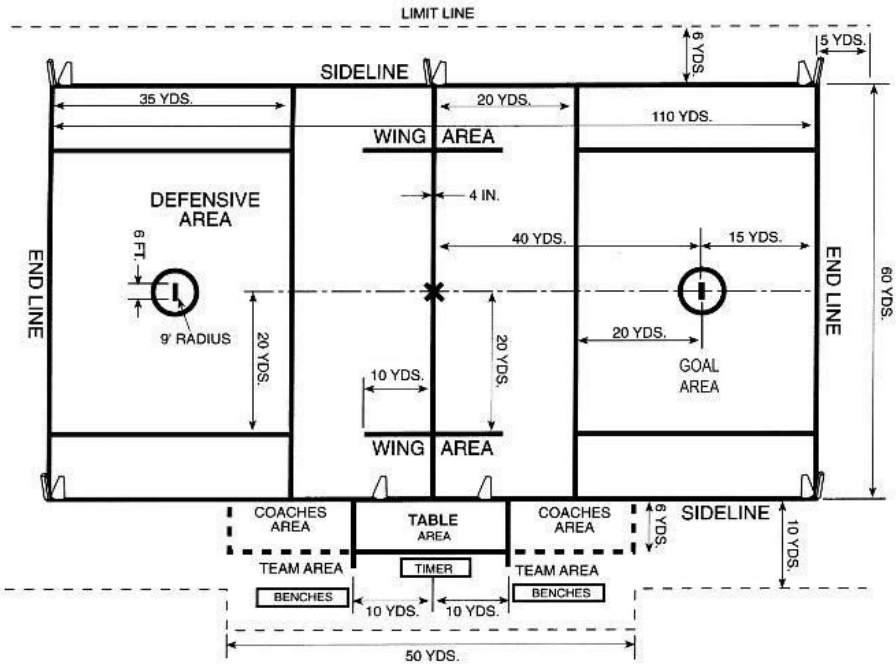

Figure 1: *Field diagram showing total distances of the men's US lacrosse regulation field (Field Diagrams, 2016).*

Lacrosse requires a high level of aerobic and anaerobic fitness, with quick starts, short bursts of sprints and longer distance runs with and without possession of the ball. Need for speed, quick direction change, and varying movements for individual positions, each add increased muscular and

cardiovascular system endurance and power requirements (Sell et al., 2018). Utilization of in-game data collection can be used to gain insight to an athlete's conditioning and readiness to perform in game situations. Analysis of player metrics can also be used to quantify an athlete's performance demands in each session, whether it is a practice or game. The internal metrics and physiological output of individual members of a lacrosse team can be monitored utilizing a commercially available team system, such as the Polar Team Pro System (PTPS), which can also allow for the collection of external metrics and movement parameters. The PTPS records time spent in designated heart rate zones, caloric expenditure, and time in defined sprint zones. The PTPS also utilizes a global positioning system (GPS) connection to measure distance traveled, speed, and distance in defined speed zones (Conners, Whitehead, Shimizu, & Bailey, 2018).

The purpose of this study was to observe and quantify the internal and external demands of high school lacrosse players during tournament game play and practice sessions. The comparison of factors including time in sprint zones, distance traveled, and heart rate between positions may highlight a need for varied conditioning and training requirements for each specific player based on their type of session. Researchers anticipated seeing elevated distances and increased durations during practice sessions as compared with games. It was also hypothesized that games caused players to show higher HR averages. In addition to the game and practice comparisons, individual positions may show different demands as well. It was anticipated that midfield would show more completed sprints than defense and attack, and it was predicted to see values indicative of higher demands, such as elevated HR and greater distances traveled, for midfields players. Regarding the specialized position, FOGO, the position was predicted to show very short bursts of speed and have data numbers indicative of high intensity with low duration and a low sprint count. In response to the opposing team's attackers, researchers expected to see defense show occasional shorter distance sprints at high speed but not for prolonged periods of time.

II. Methods

Experimental Approach to the Problem

Data were collected from a high school level team during two practices and one tournament game with a running clock. The practices lasted an average of 130.92 minutes, while the tournament game totaled 39.58 minutes. To compare for individual position demands, each player was classified as one of five positions: midfield, defense, attack, goalie, or FOGO to allow for a comparison of positional demands. The research team did not alter training or game plans, and participants were instructed to practice, scrimmage, and compete in games as they otherwise would.

Subjects

A total of thirteen male players (mean ± *SD*; 16.23 ± 1.54 years; 175.32 ± 7.72 cm; 69.89 ± 13.60 kg) from a high school, club lacrosse team participated in the study. Of the thirteen players, five defenders, two attackers, five midfielders, and a single FOGO were recorded. All subjects were volunteer participants and completed written informed consent or parental assent approved by The University of Alabama Huntsville Institutional Review Board, prior to participation.

Procedures

Internal and external factor data were recorded using the PTPS. Each subject's height, body mass, sex, date of birth and training background (based on the number of hours spent training for lacrosse per week) were recorded and then used to make their online PTPS profile. Each monitor was specifically coded using the athlete's information and assigned an identification number. Each player would keep this number for the duration of the study to ensure player metrics were accurately monitored and recorded. The monitors were placed directly on the skin of athletes' chests via an elastic strap at the beginning of each practice and game. The sensors recorded all movement from the beginning of warmups to their cool down. All measured metrics were as follows: duration, total distance, distance rate, average speed, max speed, max HR %, minimum HR % average HR %, training load, training load rate, calorie expenditure, and calorie

rate. These rates (kcal/min) were hand calculated and not recorded by the PTPS to find a relative measure in order to compare total data found in games and practices.

Statistical Analyses

Data were recorded and analyzed as mean values and standard deviations (SD) utilizing the IBM Statistical Package for the Social Sciences (SPSS) Statistics 24 for Windows (IBM Corp., Armonk, NY, USA). The overall demand for all players during a game versus during practice were compared using a paired samples *t*-test, while positional demands between attacking, midfield, defensive, and FOGO players were compared using independent samples *t*-tests. Significance was set at $p \leq .05$, two-sided *a priori* for all analyses. Effect sizes (*r*) were also calculated for each comparison (Becker, L.A. 2000.).

Cohen's Standard	*d*	r	r^2
	2.0	.707	.500
	1.9	.689	.474
	1.8	.669	.448
	1.7	.648	.419
	1.6	.625	.390
	1.5	.600	.360
	1.4	.573	.329
	1.3	.545	.297
	1.2	.514	.265
	1.1	.482	.232
	1.0	.447	.200
	0.9	.410	.168
LARGE	0.8	.371	.138
	0.7	.330	.109
	0.6	.287	.083
MEDIUM	0.5	.243	.059
	0.4	.196	.038
	0.3	.148	.022
SMALL	0.2	.100	.010
	0.1	.050	.002
	0.0	.000	.000

Figure 2: *Effect size (r) comparison with Cohen's* d *(Becker, L.A. 2000.)*

III. Results

Parameter	Practice mean ± SD	Game mean ± SD	*p*	*t*	Effect Size (r)
Duration (min)	130.92 ± 5.28	39.58 ± 00.00	$p < .001$	51.916	0.997 VL
Total Distance (m)	3957.43 ± 329.10	1848.00 ± 607.595	$p = .024$	12.599	0.907 VL
Distance Rate (m/min)	33.63 ± 7.45	46.69 ± 15.35	$p < .001$	-2.786	-0.476 M
Average Speed (km/hr)	2.05 ± .28	2.64 ± 1.03	$p = .086$	-1.955	-0.364 M
Max Speed (km/hr)	25.7315 ± 2.25	29.44 ± 5.81	$p = .051$	-2.299	-0.388 M
Sprints	9.09 ± 3.57	7.11 ± 3.98	$p = .049$	2.322	0.253 S
Average HR %	73.89 ± 5.21	84.56 ± 5.15	$p < .001$	-5.623	-0.717 VL
Max HR %	98.611 ± 2.988	101.52 ± 5.597	$p = .087$	-1.951	-0.308 M
Calories	1266.87 ± 232.21	539.333 ± 132.78	$p < .001$	10.753	0.887 VL
Calorie Rate	9.69 ± 1.81	13.63 ± 3.35	$p = .003$	-4.199	-0.590 L

Table 1: *Metrics recorded for all players for game and practice. Results are presented as mean ± SD.*

Significant differences between game and practice data were observed for the following external factors: duration, total distance, distance rate, and number of sprints ($t \geq 2.32$, $p \leq .049$, $r \geq .253$). Significant differences between games and practices were also found for the following internal factors: average HR %, training load, training load rate, calories, and calorie rate *(*$t \geq 4.2$, $p \leq .003$, $r \geq .590$). Games had a higher intensity and shorter duration than practices.

Positional comparisons between midfield and FOGO positions were found to have significant differences for max HR ($t = 2.411$, $p = .028$, $r = .525$) and number of sprints ($t = 3.242$, $p = .005$, $r = .745$). All other variables: total distance, distance rate, average speed, max speed, average HR %, training load, training load rate, calorie expenditure (kcal), and calorie rate (kcal/min) showed no other significant differences ($p > .137$). Although insignificant distance rate had a medium effect size (r = .362), max speed and average speed had medium effect sizes (r≥.300). The data found for average HR% (r = .399) and calorie rate (r = .325) also showed a medium effect size.

IV. Discussion

The purpose of the study was to quantify the differences in the physiological demand players experience between game and practice play in the sport of lacrosse as well as to analyze positional metric differences. It was hypothesized that midfield players would complete more sprints and cover greater distances than defense and attack positions as a result of their positional requirements. It also was hypothesized that the FOGO position would perform a high number of sprints but not as many as the midfield players. Attack players were expected to demonstrate consistent, fast, and powerful movements with high speed sprints in short bursts. Data was expected to show shorter distance sprints performed by defensive players.

During the game, players expended significantly fewer calories than during the practices, however the duration of the game was also significantly less. Because practices lasted 130.92 ±

5.28 and players expended 1266.87 ± 232.21 kcal, players presented a calorie rate of 9.69 ± 1.81 kcal/min. Alternatively, the game had a duration of 39.58 minutes with calories expended being 539.333 ± 132.78 kcal, resulting in a caloric expenditure rate of 13.63 ± 3.35 kcal/min. Thus, participation in games resulted in an elevated number of calories burned per minute rate compared to practices. Overall, players burned roughly half the number of calories during game competition compared to practices, which was shown to be a significant difference (p = .003) with a large effect size (r=.590). The elevated caloric expenditure rate shows that games are more physiologically demanding than practices, despite having shorter durations.

When comparing individual positions, significant differences were found between the FOGO and midfield positions for max HR and number of sprints performed. During practices and the game, midfield completed 9.5 ± 3.57 sprints while the FOGO position completed 3.50 ± 1.29 sprints. This data shows that midfield players tend to complete three times the number of sprints that the FOGO position does. This finding supported the hypothesis and was expected, since midfield players spend a greater amount of total time on the field during a game than FOGO. In another study comparing individual positions, midfielders were found to perform more sprinting when compared with attackers and defenders across all quarters (Polley, Cormack, Tim J. Gabbett, & Polglaze, 2015). The data recorded in this study showed significant differences in maximum heart rate percentage (max HR %) between positions. When taking all data into consideration, midfield data showed a mean of 99.79% of a player's predicted max HR% on average between games and practices. In addition, although not statistically significant, midfield players had the highest calorie rate (11.55 ± 2.81) versus all three other positions by the data [defense (10.18 ± 2.77), attack (9.01 ± 3.599), FOGO (9.62 ± 2.80)]. This data, despite a lack of significance, can be useful information to coaches and players regarding fueling strategies, as midfield players may require greater amounts of calories to replenish what was lost during games or practices.

As a pilot study, this investigation had a limited sample size. At only 13 subjects, it is difficult to show population significance. The limited n-size was further conflicted with inconsistent practice attendance and inclement weather, resulting in limited game data. Further, the game data was collected during a tournament, rather than a regulation game and featured a running clock, which reduced the overall playing duration that occurred.

To our knowledge, there is little research done on positional comparisons in men's lacrosse. Continued research on both men's and women's lacrosse athletes at the high school and collegiate level may lead to better knowledge of player metrics and will help athletes and coaches to better understand what conditioning levels are required for individual players at each level for games and practices. Future studies can be directed towards the expanse of knowledge of lacrosse physiological metrics and research may benefit from continued studies on male lacrosse athletes as well as the inclusion of the female athletes of the sport.

V. Practical Application

This data can be utilized to improve player performance by creating a training regimen reflecting game demands. Based on data recorded, the internal physiological metrics and the external movement metrics between game and practice can be significantly different. During the games, players show higher average HR and more sprints at faster speeds. It was shown by our data that players show a higher intensity, on average, for games than practice, encouraging a high intensity, low duration practice should coaches wish to train with close relation to games. These data also help coaches and players understand the possible variances between positional nutrition necessities showing the approximate calorie needs per player.

References

Bond, C. W., Bennett, T. W., & Noonan, B. C. (2018). Evaluation of skating top speed, acceleration, and multiple repeated sprint speed ice hockey performance tests. *The Journal of Strength & Conditioning Research*, *32*(8), 2273–2283.

Conners, R. T., Whitehead, P. N., Shimizu, T. S., & Bailey, J. D. (2018). Coaching and technology: Live team monitoring to improve training and safety. *Strategies, 31*(5), 15–20.

Enemark-Miller, E. A., Seegmiller, J. G., & Rana, S. R. (2009). Physiological profile of women's lacrosse players. *The Journal of Strength & Conditioning Research*, *23*(1), 39–43.

Making the fastest game on two feet faster. (2016, June 7). *USLacrosse.org.* https://www.uslacrosse.org/blog/making-the-fastest-game-on-two-feet-faster.

Polley, C. S., Cormack, S. J., Gabbett, T. J., & Polglaze, T. (2015). Activity profile of high-level australian lacrosse players. *Journal of Strength and Conditioning Research* 29(1), 126–36.

Sapp, R. M., Aronhalt, L., Landers-Ramos, R. Q., Spangenburg, E. E., Wang, M. Q., & Hagberg, J. M. (2017). Laboratory and match physiological data from an elite male collegiate soccer athlete. *The Journal of Strength & Conditioning Research*, *31*(10), 2645–2651.

Scroggs, W. (2018). The game, field and equipment. *2019 and 2020 NCAA Men's Lacrosse Rules and Interpretations* (pp. 8–13). National Collegiate Athletic Association.

Sell, K. M., Prendergast, J. M., Ghigiarelli, J. J., Gonzalez, A. M., Biscardi, L. M., Jajtner, A. R., & Rothstein, A. S. (2018). Comparison of physical fitness parameters for starters vs. nonstarters in an NCAA division I men's lacrosse team. *The Journal of Strength & Conditioning Research*, *32*(11), 3160–3168.

Steinhagen, M. R., Meyers, M. C., Erickson, H. H., Noble, L., & Richardson, M. T. (1998). Physiological profile of college club-sport lacrosse athletes. *The Journal of Strength & Conditioning Research*, *12*(4), 226–231.

US Lacrosse 2017 Participation Survey. (2017). www.uslacrosse.org website: https://www.uslacrosse.org/sites/default/files/public/documents/about-us-lacrosse/participation-survey-2017.pdf

US Lacrosse. "Field Diagrams," July 22, 2016. https://www.uslacrosse.org/rules/field-diagrams.

THE UNIVERSITY OF
ALABAMA IN HUNTSVILLE

PERPETUA